

Figure 3 MALDI-TOF mass spectra of the free peptides and mixtures of the peptides and RRE RNA or RRE C46G74 RNA. (A) DLA peptide (B) DLA peptide-RRE RNA (C) DLA peptide-RRE C46G74 RNA (D) RLA peptide (E) RLA peptide-RRE RNA (F) RLA peptide-RRE C46G74 RNA. This figure is available in colour online at www.interscience.wiley.com/journal/jpepsci.

to the RLA peptide did not disappear upon addition of the RRE mutant (Figure 3(F)), showing that specific RNA–polypeptide interactions with a K_d of at least more than 30 nM could be analyzed by this method. As expected, addition of the wild-type and mutant RRE to the λ N peptide, which does not bind specifically to the RRE, resulted in no change in the peptide signal (Figure S2, supporting data).

In order to confirm that specific binding of the λ N peptide with the boxB RNA could also be observed by this method, the interaction of the DLA, and RLA, and λ N peptides with the wild-type boxB and a mutant boxB was analyzed (Figures 4 and S3, supporting data). Addition of the wild-type and mutant boxB RNAs to the DLA and RLA peptides resulted in the retention of the signals corresponding to the peptides (Figure S3(A)–(F), supporting data). On the other hand, addition of the wild-type box B to the λ N peptide resulted in an almost complete disappearance of the signal corresponding to

the peptide, while the addition of the mutant boxB (G8A) did not affect the peptide signal (Figure 4). This further confirmed that specific RNA–polypeptide binding could be simply detected by whether or not the free-peptide signal in the MALDI-TOF MS vanishes upon RNA addition.

Identification of Specific RNA-binding Peptides from a Simple Peptide Library

In order to elucidate the utility of the present technique to identify RNA-binding peptides from mixtures of peptides with varying RNA-binding affinities, mixtures of peptides were treated with either the RRE or the RRE mutant (Figure 5). As a result, for example, when the DLA, RLA and λ N peptides were mixed with the RRE, only the signals corresponding to the DLA and RLA peptide disappeared (Figure 5(B)), while both the signals were present when the RRE mutant was used (Figure 5(C)).

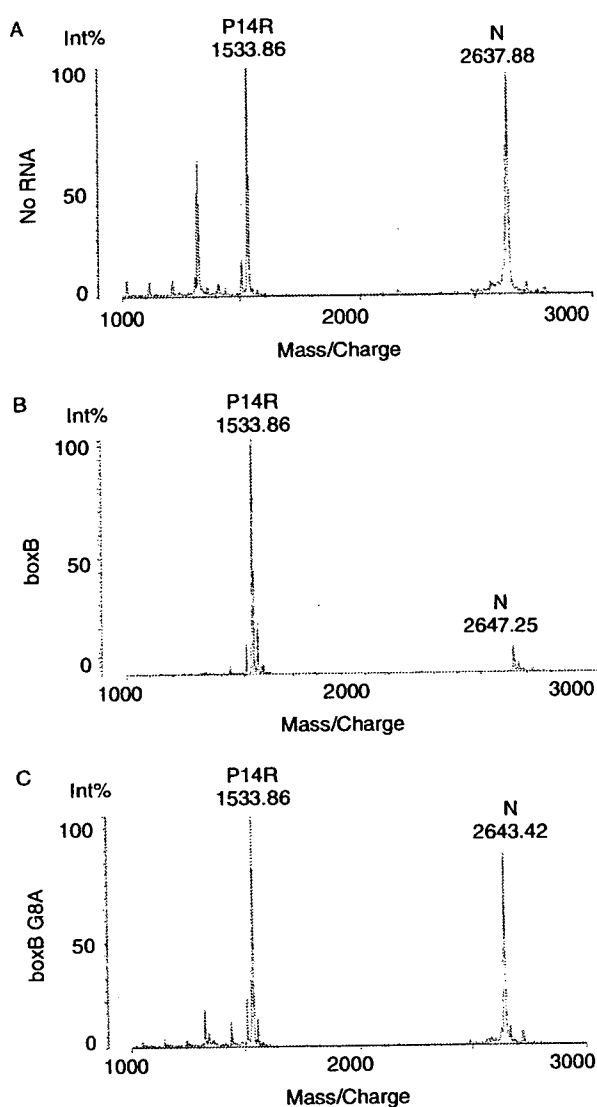


Figure 4 MALDI-TOF mass spectra of the free peptide and mixtures of the peptide and boxB RNA or boxB G8A RNA. (A) λ N peptide (B) λ N peptide-boxB RNA (C) λ N peptide-boxB G8A RNA. This figure is available in colour online at www.interscience.wiley.com/journal/jpepsci.

CONCLUSIONS

A simple method for detecting specific RNA–polypeptide interactions by MALDI-TOF MS that avoids difficulties associated with the direct analysis of the RNA–polypeptide complex, and is expected to be useful in the qualitative analysis of RNA–polypeptide interactions is described. The ability to identify strongly binding peptides from a mixture of similar peptides with varying RNA affinity, combined with the ease with which analysis can be carried out, suggests that MALDI-TOF MS may be applicable for the high-throughput screening of specific RNA-binder from simple peptide libraries.

MATERIALS AND METHODS

The Preparation of RNAs and Peptides

The RNAs were prepared by *in vitro* transcription using T7 RNA polymerase of synthetic oligonucleotide templates for RRE (5'-GGCCTGTACCGTCAGCTTGCCTGCGCCAGACCTATAG-TGAGTCGTATTAC-3'), RRE C46G74 (5'-GGCCTTACCCTGCA-GCTTGCCTGCGCCAGACCTATAGTGTGAGTCGTATTAC-3'), boxB (5'-GGGCCCTTCTTCAGGGCCCTATAGTGTGAGTCGTATTAC-3'), and boxB G8A (5'-GGGCCCTTCTTTAGGGCCCTATAGTGTGAGTCGTATTAC-3') that were annealed to the T7 primer (5'-GTAATACGACTCACTATA-3'). The RNA oligonucleotides were purified in denaturing PAGE, and desalted on a NAP 5 columns (Amersham Biosciences). The RNA was dissolved in H₂O to 100 pmol/ μ l, and were annealed by heating at 95°C for 5 min and quick-cooling to 0°C. The arginine-rich peptides were constructed on XX resin using automatic peptide synthesizer (Applied Biosystems, Model 433A) starting from Fmoc-Arg(pmc)-resin (0.25 mmol/g) with standard Fmoc-chemistry. The peptides were deprotected and cleaved from the resin by the treatment with TFA for 4 h at room temperature. The peptides were isolated and purified by HPLC with linear gradient conditions of acetonitrile/H₂O/0.1% TFA as eluent. The peptides were lyophilized as fluffy white powder of the acetates and analyzed by MALDI-TOF MS using Voyager Linear II. The [M + H] cations were detected for all synthetic peptides. The λ N peptide used in this study was shorter by four amino acid residues at C-terminal than that used for gel shift (Figure 1). These amino acid residues are not important for binding to boxB RNA [14].

Mass Spectrometric Analysis

The matrices CHCA, DHB, 3-HPA were obtained from SIGMA-ALDRICH, and 2,4,6-THAP was obtained from Fluka. Ammonium citrate was obtained from SIGMA-ALDRICH.

One microliter of the RNA and 1 μ l of the peptide (100 pmol/ μ l in H₂O), in the case of the mixtures of RRE or RRE C46G74 RNAs and all peptides, 3 μ l of the RNA (100 pmol/ μ l) and 0.1 μ l of the peptide (1 nmol/ μ l in H₂O) were incubated together in a 1.5-ml tube for 10 min at room temperature (20°C) or on ice. Following the addition of 0.5 μ l of 0.2 N ammonium citrate and 0.5 μ l of ProteoMass P14R MALDI-MS Standard (SIGMA-ALDRICH), each sample was dropped on a sample plate. Then, the matrix solution 1.2 μ l of 20 mg/ml 2,4,6-THAP in methanol, 1 μ l of 15 mg/ml DHB in 0.1% TFA/acetonitrile (2:1) or 1.2 μ l of 60 mg/ml 3-HPA in H₂O, was dropped on the sample very carefully, and dried. After drying the spots on the plate completely, the mass analysis performed with Axima CFRplus MALDI-TOF MS spectrometer (Shimadzu, Japan). Each spectrum was averaged for 100 laser shots in linear mode at 120 mV.

RNA-peptides Binding Assay *In Vivo*

pBR plasmid DNAs activities were monitored using the LacZ colony color assay [2] with N567/reporter cells containing pAC-RRE or pAC- λ nut plasmids. N567/pAC cells (50 μ l) were transformed using 1 μ l of the pBR plasmid DNA (10 ng) by heat shock, and incubated in the tryptone medium (0.5 ml) at 37°C for 1 h. A portion of the culture was spread onto

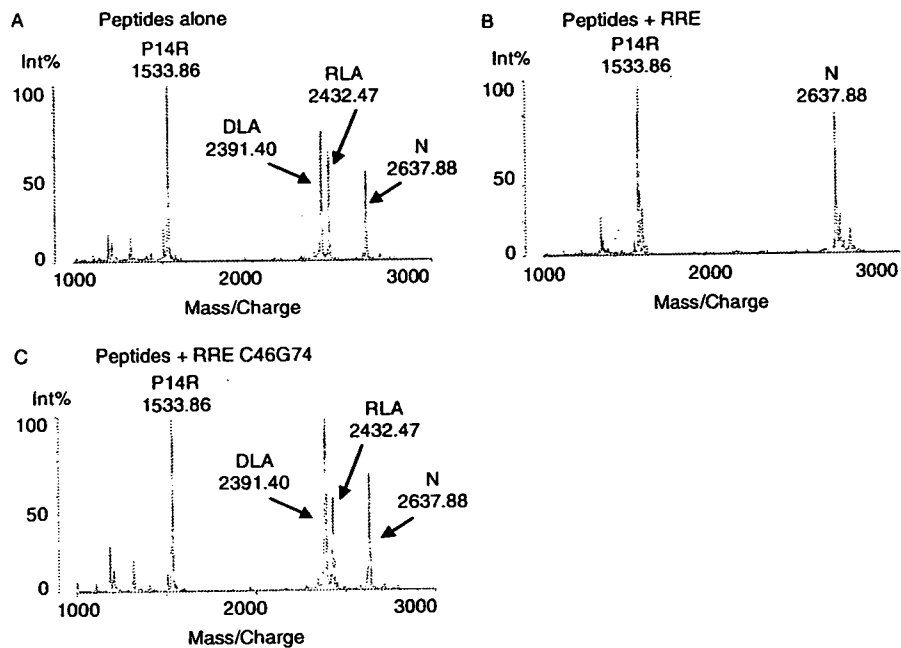


Figure 5 MALDI-TOF mass spectra of mixed peptides and RRE RNA or RRE C46G74 RNA. (A) DLA, RLA, and λ N peptides (B) DLA, RLA, and λ N peptides-RRE RNA (C) DLA, RLA, and λ N peptides-RRE C46G74 RNA. This figure is available in colour online at www.interscience.wiley.com/journal/jpepsci.

tryptone plates (60 mm diameter) containing 100 μ g/ml ampicillin, 20 μ g/ml chloramphenicol, 0.05 mM IPTG, 80 μ g/ml 5-bromo-4-chloro-3-indolyl- β -D-galactopyranoside (X-gal), incubated at 37 °C for 24 h, and the proportion of blue colonies was scored [2].

Supplementary Material

Supplementary electronic material for this paper is available in Wiley InterScience at: <http://www.interscience.wiley.com/jpages/1075-2617/suppmat/>

Acknowledgements

This work was supported in part by a Grant-in-Aid Research in Priority Areas from the Ministry of Education, Culture, Sports, Science and Technology (MEXT) of Japan, and by 'High-Tech Research Center' Project for private universities: matching fund subsidy from MEXT (2004-2008).

REFERENCES

1. SenGupta DJ, Zhang B, Kraemer B, Pochart P, Fields S, Wickens M. A three-hybrid system to detect RNA-protein interactions in vivo. *Proc. Natl. Acad. Sci. U.S.A.* 1996; **93**: 8496-8501.
2. Harada K, Martin SS, Frankel AD. Selection of RNA-binding peptides in vivo. *Nature* 1996; **380**: 175-179.
3. Thomas B, Akoulitchev AV. Mass spectrometry of RNA. *Trends Biochem. Sci.* 2006; **31**: 173-181.
4. Shaler TA, Wickham JN, Sannes KA, Wu KJ, Becker CH. Effect of impurities on the matrix-assisted laser desorption mass spectra of single-stranded oligodeoxynucleotides. *Anal. Chem.* 1996; **68**: 576-579.
5. Wu KJ, Steding A, Becker CH. Matrix-assisted laser desorption time-of-flight mass spectrometry of oligonucleotides using 3-hydroxycyclohexanoic acid as an ultraviolet-sensitive matrix. *Rapid Commun. Mass Spectrom.* 1993; **7**: 142-146.
6. Pielek U, Zürcher W, Schär M, Moser HE. Matrix-assisted laser desorption ionization time-of-flight mass spectrometry: a powerful tool for the mass and sequence analysis of natural and modified oligonucleotides. *Nucleic Acids Res.* 1993; **21**: 3191-3196.
7. Zhu YF, Chung CN, Taranenco NI, Allman SL, Martin SA, Haff L, Chen CH. The study of 2,3,4-trihydroxyacetophenone and 2,4,6-trihydroxyacetophenone as matrices for DNA detection in matrix-assisted laser desorption/ionization time-of-flight mass spectrometry. *Rapid Commun. Mass Spectrom.* 1996; **10**: 383-388.
8. Kirpekar F, Nordhoff E, Kristiansen K, Roepstorff P, Lezius A, Hahner S, Karas M, Hillenkamp F. Matrix assisted laser desorption/ionization mass spectrometry of enzymatically synthesized RNA up to 150 kDa. *Nucleic Acids Res.* 1994; **22**: 3866-3870.
9. Thiede B, von Janta-Lipinski M. Noncovalent RNA-peptide complexes detected by matrix-assisted laser desorption/ionization mass spectrometry. *Rapid Commun. Mass Spectrom.* 1998; **12**: 1889-1894.
10. Sugaya M, Nishino N, Katoh A, Harada K. Amino acid requirements for the high affinity binding of a selected arginine-rich peptide with the HIV Rev-response element RNA. *J. Pept. Sci.* 2008 (in press).
11. Tan R, Frankel AD. Structural variety of arginine-rich RNA-binding peptides. *Proc. Natl. Acad. Sci. U.S.A.* 1995; **92**: 5282-5286.
12. Beavis RC. Matrix-assisted ultraviolet laser desorption: evolution and principles. *Org. Mass Spectrom.* 1992; **27**: 653-659.
13. Tang K, Allman SL, Chen CH. Matrix-assisted laser desorption ionization of oligonucleotides with various matrices. *Rapid Commun. Mass Spectrom.* 1993; **7**: 943-948.
14. Franklin NC. Clustered arginine residues of bacteriophage λ N protein are essential to antitermination of transcription, but their locale cannot compensate for *boxB* loop defects. *J. Mol. Biol.* 1993; **231**: 343-360.

HEPATOLOGY

Inhibition of hepatitis C virus infection and expression *in vitro* and *in vivo* by recombinant adenovirus expressing short hairpin RNA

Naoya Sakamoto,^{*,†} Yoko Tanabe,^{*} Takanori Yokota,[‡] Kenichi Satoh,[§] Yuko Sekine-Osajima,^{*} Mina Nakagawa,^{*,†} Yasuhiro Itsui,^{*} Megumi Tasaka,^{*} Yuki Sakurai,^{*} Chen Cheng-Hsin,^{*} Masahiko Yano,[¶] Shogo Ohkoshi,[¶] Yutaka Aoyagi,[¶] Shinya Maekawa,^{**} Nobuyuki Enomoto,^{**} Michinori Kohara[§] and Mamoru Watanabe^{*}

Departments of ^{*}Gastroenterology and Hepatology, [†]Hepatitis Control, and [‡]Neurology and Neurological Science, Tokyo Medical and Dental University, [§]Department of Microbiology and Cell Biology, The Tokyo Metropolitan Institute of Medical Science, Tokyo, [¶]Gastroenterology and Hepatology Division, Graduate School of Medical and Dental Sciences, Niigata University, Niigata, and ^{**}First Department of Medicine, Yamanashi University, Yamanashi, Japan

Key words

adenovirus vector, hepatitis C virus, RNA interference.

Accepted for publication 12 April 2007.

Correspondence

Dr Naoya Sakamoto, Department of Gastroenterology and Hepatology, Tokyo Medical and Dental University, 1-5-45 Yushima, Bunkyo-ku, Tokyo 113-8519, Japan.
Email: nsakamoto.gast@tmd.ac.jp

NS and YT have contributed equally to this paper.

Abstract

Background and Aim: We have reported previously that synthetic small interfering RNA (siRNA) and DNA-based siRNA expression vectors efficiently and specifically suppress hepatitis C virus (HCV) replication *in vitro*. In this study, we investigated the effects of the siRNA targeting HCV-RNA *in vivo*.

Methods: We constructed recombinant retrovirus and adenovirus expressing short hairpin RNA (shRNA), and transfected into replicon-expressing cells *in vitro* and transgenic mice *in vivo*.

Results: Retroviral transduction of Huh7 cells to express shRNA and subsequent transfection of an HCV replicon into the cells showed that the cells had acquired resistance to HCV replication. Infection of cells expressing the HCV replicon with an adenovirus expressing shRNA resulted in efficient vector delivery and expression of shRNA, leading to suppression of the replicon in the cells by $\sim 10^{-3}$. Intravenous delivery of the adenovirus expressing shRNA into transgenic mice that can be induced to express HCV structural proteins by the Cre/loxP switching system resulted in specific suppression of virus protein synthesis in the liver.

Conclusion: Taken together, our results support the feasibility of utilizing gene targeting therapy based on siRNA and/or shRNA expression to counteract HCV replication, which might prove valuable in the treatment of hepatitis C.

Introduction

Hepatitis C virus (HCV), which affects 170 million people worldwide, is one of the most important pathogens causing liver-related morbidity and mortality.¹ The difficulty in eradicating HCV is attributable to limited treatment options against the virus and their unsatisfactory efficacies. Even with the most effective regimen with pegylated interferon (IFN) and ribavirin in combination, the efficacies are limited to less than half of the patients treated.² Given this situation, the development of safe and effective anti-HCV therapies is one of our high-priority goals.

RNA interference (RNAi) is a process of sequence-specific, post-transcriptional gene silencing that is initiated by double-stranded RNA.^{3,4} Because of its potency and specificity, RNAi rapidly has become a powerful tool for basic research to analyze gene functions and for potential therapeutic applications. Recently,

successful suppression of various human pathogens by RNAi have been reported, including human immunodeficiency viruses,^{5,6} poliovirus,⁷ influenza virus,⁸ severe acute respiratory syndrome (SARS) virus⁹ and hepatitis B virus (HBV).¹⁰⁻¹³

We and other researchers have reported that appropriately designed small interfering RNA (siRNA) targeting HCV genomic RNA can efficiently and specifically suppress HCV replication *in vitro*.¹⁴⁻¹⁹ We have tested siRNA designed to target the well-conserved 5'-untranslated region (5'-UTR) of HCV-RNA, and identified the most effective target, just upstream of the translation initiation codon. Furthermore, transfection of DNA-based vectors expressing siRNA was as effective as that of synthetic siRNA in suppressing HCV replication.¹⁴

In this study, we explored the further possibility that efficient delivery and expression of siRNA may be effective in suppression and elimination of HCV replication and that delivery of such

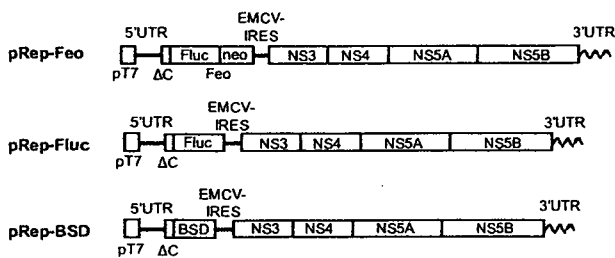


Figure 1 Structures of HCV replicon plasmids. The pRep-Feo expressed a chimeric reporter protein of firefly luciferase (Fluc) and neomycin phosphotransferase (GenBank accession No. AB119282).^{14,20} The pRep-Fluc expressed the Fluc protein. The pRep-BSD expressed the blasticidin S (BSD) resistance gene. pT7, T7 promoter; 5'UTR, HCV 5'-untranslated region; ΔC, truncated HCV core region (nt. 342–377); neo, neomycin phosphotransferase gene; EMCV, encephalomyocarditis virus; NS3, NS4, NS5A and NS5B, genes that encode HCV non-structural proteins; 3'UTR, HCV 3'-untranslated region.

HCV-directed siRNA *in vivo* may be effective in silencing viral protein expression in the liver. Here, we report that HCV replication was suppressed *in vitro* by recombinant retrovirus and adenovirus vectors expressing short hairpin RNA (shRNA) and that the delivery of the adenovirus vector to mice *in vivo* specifically inhibited viral protein synthesis in the liver.

Methods

Cells and cell culture

Huh7 and Retro Pack PT67 cells (Clontech, Palo Alto, CA, USA) were maintained in Dulbecco's modified minimal essential medium (Sigma, St. Louis, MO, USA) supplemented with 10% fetal calf serum at 37°C under 5% CO₂. To maintain cell lines carrying the HCV replicon, G418 (Wako, Osaka, Japan) was added to the culture medium to a final concentration of 500 μg/mL.

HCV replicon constructs and transfection

HCV replicon plasmids, pRep-Feo, pRep-Fluc and pRep-BSD were constructed from a virus, HCV-N strain, genotype 1b.²¹ The pRep-Feo expressed a chimeric reporter protein of firefly luciferase (Fluc) and neomycin phosphotransferase.^{14,20} The pRep-Fluc and the pRep-BSD expressed the Fluc and blasticidin S (BSD) resistance genes, respectively (Fig. 1). The replicon RNA synthesis and the transfection protocol have been described previously.²²

Synthetic siRNA and siRNA-expression plasmid

The design and construction of HCV-directed siRNA vectors have been described.¹⁴ Briefly, five siRNA targeting the 5'-UTR of HCV RNA were tested for their efficiency to inhibit HCV replication, and the most effective sequence, which targeted nucleotide position of 331 though 351, was used in the present study. To construct shRNA-expressing DNA cassettes, oligonucleotide inserts were synthesized that contained the loop sequence (5'-TTC AAG AGA-

3') flanked by sense and antisense siRNA sequences (Fig. 2a). These were inserted immediately downstream of the human U6 promoter. To avoid a problem in transcribing shRNA because of instability of the DNA strands arising from the tight palindrome structure, several C-to-T point mutations, which retained completely the silencing activity of the shRNA, were introduced into the sense strand of the shRNA sequences (referred to as 'm').²³ A control plasmid, pUC19-shRNA-Control, expressed shRNA directed towards the Machado–Joseph disease gene, which is a mutant of ataxin-3 gene and is not normally expressed. We have previously described the sequence specific activity of the shRNA-Control.²⁴

Prior to construction of the virus vectors, we tested silencing efficiency of five shRNA constructs of different lengths that covered the target sequence (Fig. 2a). The shRNA-HCV-19, shRNA-HCV-21 and shRNA-HCV-27 had target sequences of 19, 21 and 27 nucleotides, respectively. Transfection of these shRNA constructs into Huh7/pRep-Feo showed that shRNA with longer target sequences had better suppressive effects (Fig. 2b). Therefore, we used shRNA-HCV-27m (abbreviated as shRNA-HCV) in the following study.

Recombinant retrovirus vectors

The U6-shRNA expression cassettes were inserted into the *Sma*I/*Hind*III site of a retrovirus vector, pLNCX2 (Clontech) to construct pLNCshRNA-HCV and pLNCshRNA-Control (Fig. 2c). The plasmids were transfected into the packaging cells, Retro Pack PT67. The culture supernatant was filtered and added onto Huh7 cells with 4 μg/mL of polybrene. Huh7 cell lines stably expressing shRNA were established by culture in the presence of 500 μg/mL of G418.

Recombinant adenovirus

Recombinant adenoviruses expressing shRNA were constructed using an Adenovirus Expression Vector Kit (Takara, Otsu, Japan). The U6-shRNA expression DNA cassette was inserted into the *Swa*I site of pAxcw to construct pAxshRNA-HCV and pAxshRNA-Control. The adenoviruses were propagated according to the manufacturer's protocol (AxshRNA-HCV and AxshRNA-Control; Fig. 2c). A 'multiplicity of infection' (MOI) was used to standardize infecting doses of adenovirus. The MOI stands for the ratio of infectious virus particles to the number of cells being infected. An MOI = 1 represents equivalent dose to introduce one infectious virus particle to every host cell that is present in the culture.

Plasmids for assays of interferon responses

pISRE-TA-Luc (Invitrogen, Carlsbad, CA, USA) contained five copies of the consensus interferon stimulated response element (ISRE) motifs upstream of the Fluc gene. pTA-Luc (Invitrogen), which lacks the enhancer element, was used for background determination. The pcDNA3.1 (Invitrogen) was used as an empty vector for mock transfection. pRL-CMV (Promega, Madison, WI, USA), which expresses the *Renilla* luciferase protein, was used for normalization of transfection efficiency.²⁵ A plasmid, pEGFPneo (Invitrogen), was used to monitor percentages of transduced cells.

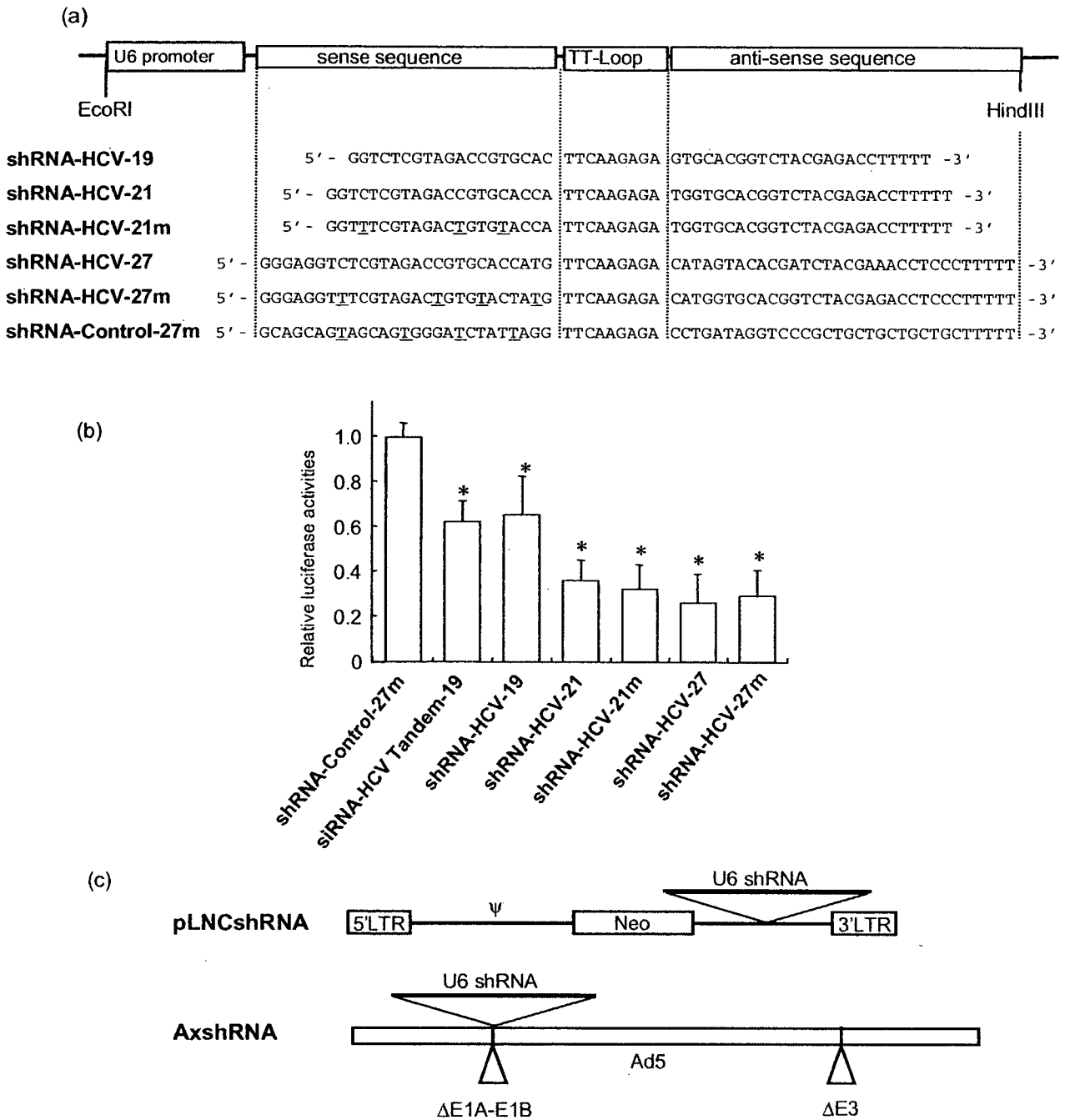


Figure 2 Structure of shRNA-expression constructs and shRNA sequences. (a) Structure of shRNA-expression cassette and shRNA sequences. TT-Loop, the loop sequence. The shRNA-Control was directed toward an unrelated target, Machado–Joseph disease gene. Underlined letters indicate C-to-T point mutations in the sense strand. (b) The shRNA-expression plasmids were transfected into Huh7/pRep-Feo cells, and internal luciferase activities were measured at 48 h of transfection. Each assay was done in triplicate, and the values are displayed as mean + SD. **P* < 0.05. (c) pLNCshRNA, structure of a recombinant retrovirus expressing shRNA. Ψ, the retroviral packaging signal sequence. AxshRNA, structure of a recombinant adenovirus expressing shRNA.

Real-time RT-PCR analysis

Total cellular RNA was extracted from cultured cells or liver tissue using ISOGEN (Nippon Gene, Tokyo, Japan). Total cellular RNA (2 µg) was used to generate cDNA from each sample using the SuperScript II reverse-transcriptase (Invitrogen). The mRNA expression levels were measured using the Light Cycler PCR and detection system (Roche, Mannheim, Germany) and Light Cycler Fast Start DNA Master SYBR Green I mix (Roche).

Luciferase assays

Luciferase activity was measured using a luminometer, Lumat LB9501 (Promega) and the Bright-Glo Luciferase Assay System (Promega) or the Dual-Luciferase Reporter Assay System (Promega).

Northern and western hybridization

Total cellular RNA was separated by denaturing agarose-formaldehyde gel electrophoresis, and transferred to a nylon membrane. The membrane was hybridized with a digoxigenin-labeled probe specific for the full-length replicon sequence, and subsequently with a probe specific for beta-actin. The signals were detected by chemiluminescence reaction using a Digoxigenin Luminescent Detection Kit (Roche), and visualized by Fluoro-Imager (Roche). For the western blotting, 10 µg of total cell lysate was separated on NuPAGE 4.12% Bis-TrisGel (Invitrogen), and blotted onto an Immobilon PVDF Membrane (Roche). The membrane was incubated with monoclonal antibodies specific for HCV-NS5A (BioDesign, Saco, ME, USA), NS4A (Virogen, Watertown, MA, USA), or beta-actin (Sigma), and detected by a chemiluminescence reaction (BM Chemiluminescence Blotting Substrate; POD, Roche).

Transient-replication assays

A replicon, pRep-Fluc, was transfected into cells and the luciferase activities of the cell lysates were measured serially. To correct the transfection efficiency, each value was divided by the luciferase activity at 4 h after the transfection.

Stable colony formation assays

Cells were transfected with a replicon, pRep-BSD, and were cultured in the presence of 150 µg/mL of BSD (Invitrogen). BSD-resistant cell colonies appeared after ~3 weeks of culture, and were counted.

HCV-JFH1 virus cell culture

An *in-vitro* transcribed HCV-JFH1 RNA²⁶ was transfected into Huh7.5.1 cells.²⁷ Naive Huh7.5.1 cells were subsequently infected by the culture supernatant of the JFH1-RNA transfected Huh-7.5.1 cells, and subjected to siRNA or drug treatments. Replication levels of HCV-RNA were quantified by the realtime RT-PCR by using primers that targeted HCV-NS5B region, HCV-JFH1 sense: 5'-TCA GAC AGA GCC TGA GTC CA-3', and HCV-JFH1 antisense: 5'-AGT TGC TGG AGG GCT TCT GA-3'.

Mice and adenovirus infection

Transgenic mice, CN2-29, inducibly express mRNA for the HCV structural proteins (genotype1b, nucleotides 294–3435) by the *Cre/loxP* switching system.²⁸ The transgene does not contain full-length HCV 5'-UTR, but shares the target sequence of the shRNA-HCV. Although the transgenic mouse CN2 has been previously reported as expressing higher levels of the viral proteins, the expression levels of the viral core protein in the CN2-29 mice are modest and similar to that in the liver of HCV patients. Thus, we chose CN2-29 mice in the present study.

The mice were infected with AxshRNA-HCV or controls (AxshRNA-Control or AxCAw1) in combination with AxCAN-Cre, which expressed Cre recombinase. Three days after the infection, the mice were killed and HCV core protein in the liver was measured as described below. The BALB/c mice were maintained in the Animal Care Facility of Tokyo Medical and Dental University, and transgenic mice were in the Tokyo Metropolitan Institute of Medical Science. Animal care was in accordance with institutional guidelines. The review board of the university approved our experimental animal studies and all experiments were approved by the institutional animal study committees.

Measurement of HCV core protein in mouse liver

The amounts of HCV core protein in the liver tissue from the mice was measured by a fluorescence enzyme immunoassay (FEIA)²⁹ with a slight modification. Briefly, the 5F11 monoclonal anti-HCV-core antibody was used as the first antibody on the solid phase, and the 5E3 antibody conjugated with horseradish peroxidase was the second antibody. This FEIA can detect as little as 4 pg/mL of recombinant HCV-core protein. Contents of the HCV core protein in the liver samples were normalized by the total protein contents and expressed as pg/mg total protein.

Immunohistochemical staining

Liver tissue was frozen with optimal cutting temperature (OTC) compound (Tissue Tek; Sakura Finetechnical, Tokyo, Japan). The sections (8 µm thick) were fixed with a 1:1 solution of acetone : methanol at -20°C for 10 min and then washed with phosphate-buffered saline (PBS). Subsequently, the sections were incubated with the IgG fraction of an anti-HCV core rabbit polyclonal antibody (RR8)²⁸ in blocking buffer or antialbumin rabbit polyclonal antibody (Dako Cytomation, Glostrup, Denmark) in PBS overnight at 4°C. The sections were incubated with secondary antibody, Alexa-antirabbit IgG (Invitrogen) or TRITIC-antirabbit IgG (Sigma), for 2 h at room temperature. Fluorescence was observed using a fluorescence microscope.

Statistical analyses

Statistical analyses were performed using Student's *t*-test; *P*-values of less than 0.05 were considered to be statistically significant.

Results

Retrovirus transduction of shRNA can protect from HCV replication

Retrovirus vectors propagated from pLNCshRNA-HCV and pLNCshRNA-Control were used to infect Huh7 cells, and cell lines were established that constitutively express shRNA-HCV and shRNA-Control (Huh7/shRNA-HCV and Huh7/shRNA-Control, respectively). There were no differences in the cell morphology or growth rate between shRNA-transduced and non-transduced Huh7 cells (data not shown). The HCV replicon, pRep-Fluc, was transfected into Huh7/shRNA-HCV, Huh7/shRNA-Control and naive Huh7 cells by electroporation. In Huh7/shRNA-Control and naive Huh7 cells, the initial luciferase activity at 4 h decreased temporarily, which represents decay of the transfected replicon RNA, but increased again at 48 h and 72 h, which demonstrate *de novo* synthesis of the HCV replicon RNA. In contrast, transfection into Huh7/shRNA-HCV cells resulted in a decrease in the initial luciferase activity, reaching background by 72 h (Fig. 3a). Similarly, transfection of the replicon, pRep-BSD, into Huh7 cells and BSD selection yielded numerous BSD-resistant colonies in the naive Huh7 (832 colonies) and Huh7/shRNA-Control cell lines (740 colonies), while transfection of Huh7/shRNA-HCV, which expressed shRNA-HCV, yielded obviously fewer colonies (five colonies), indicating reduction of colony forming units by $\sim 10^2$ (Fig. 3b). There was no difference in shape, growth or viability between cells expressing the shRNA or not. These results indicated that cells expressing HCV-directed shRNA following retrovirus transduction acquired resistance to HCV replication.

Effect of recombinant adenoviruses expressing shRNA on *in vitro* HCV replication

We investigated subsequently the effects of recombinant adenovirus vectors expressing shRNA. AxshRNA-HCV and AxshRNA-Control were used separately to infect Huh7/pRep-Feo cells, and the internal luciferase activities were measured sequentially (Fig. 4a). AxshRNA-HCV caused continuous suppression of HCV RNA replication. Six days postinfection, the luciferase activities fell to background levels. In contrast, the luciferase activities of the Huh7/pRep-Feo cells infected with AxshRNA-Control did not show any significant changes compared with untreated Huh7/pRep-Feo cells (Fig. 4a). The dimethylthiazol carboxymethoxyphenyl sulfophenyl tetrazolium (MTS) assay showed no significant difference between cells that were infected by recombinant adenovirus and uninfected cells (Fig. 4b). In the northern blotting analysis, the cells were harvested 6 days after infection with the adenovirus at an MOI of 1. Feo-replicon RNA of 9.6 kb, which was detectable in the untreated Huh7/pRep-Feo cells and in the cells infected with AxshRNA-Control, diminished substantially following infection with the AxshRNA-HCV (Fig. 4c). Densitometries showed that the intracellular levels of the replicon RNA in the Huh7/pRep-Feo cells correlated well with the internal luciferase activities. Similarly in the western blotting, cells were harvested 6 days after infection with adenovirus. Levels of the HCV NS4A and NS5A proteins that were translated from the HCV replicon decreased following infection with the AxshRNA-HCV

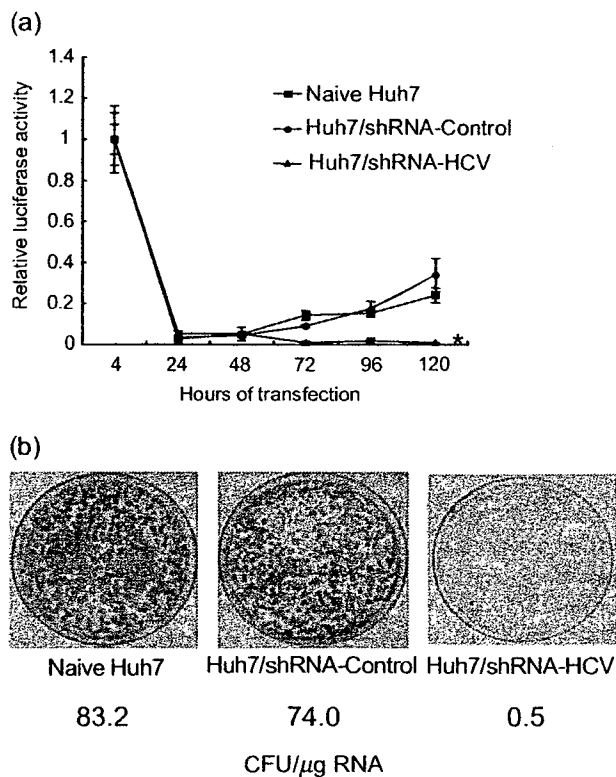
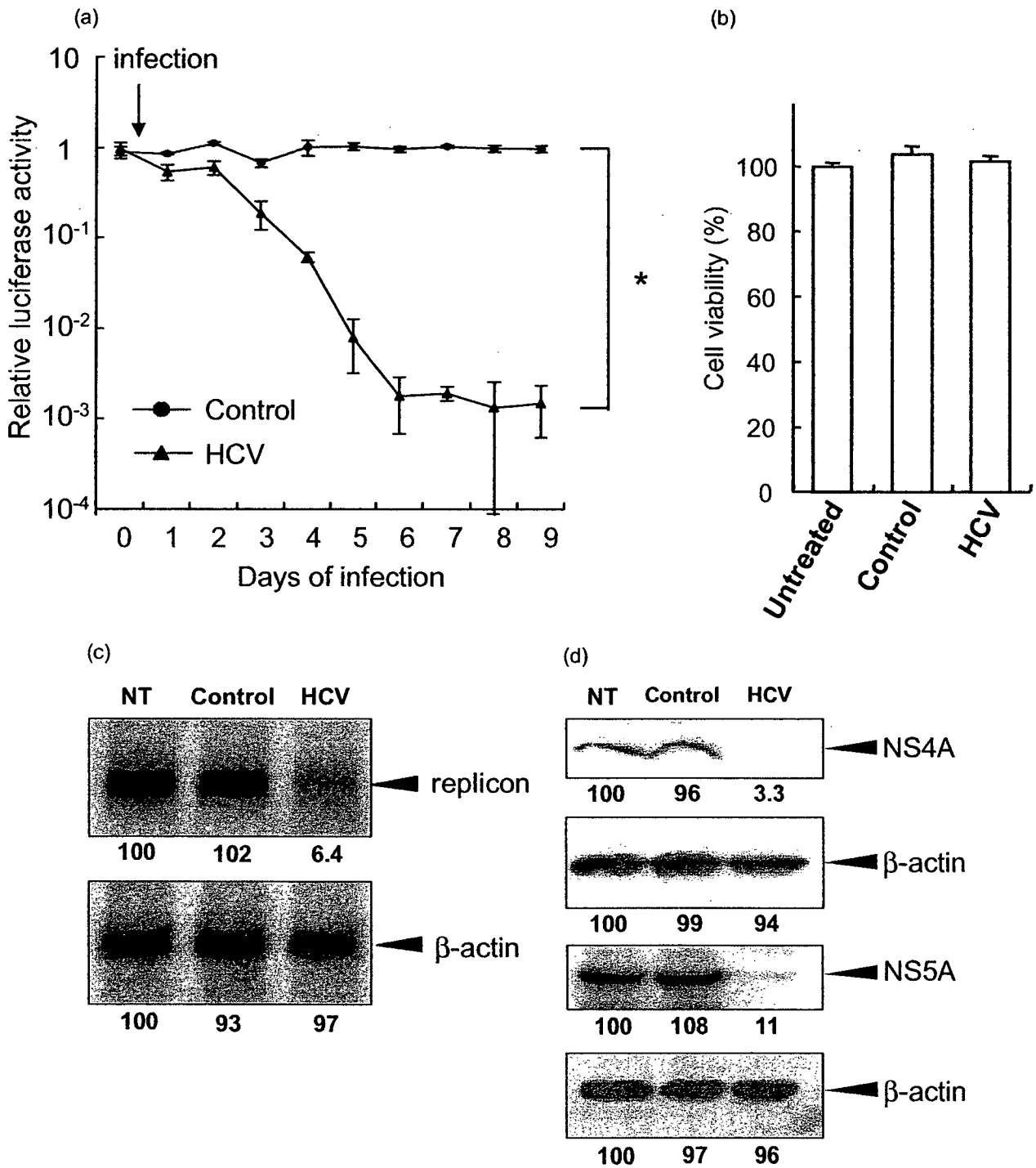


Figure 3 HCV replication can be inhibited by shRNA-HCV which was stably transfected into cells. Huh7/shRNA-HCV and Huh7/shRNA-Control stably express shRNA-HCV or shRNA-Control, respectively, following retroviral transduction. (a) Transient replication assay. An HCV replicon RNA, pRep-Fluc, was transfected into naive Huh7, Huh7/shRNA-HCV and Huh7/shRNA-Control cells. Luciferase activities of the cell lysates were measured serially at the times indicated, and the values were plotted as ratios relative to luciferase activities at 4 h. The luciferase activities at 4 h represent transfected replicon RNA. The data are mean \pm SD. An asterisk denotes a *P*-value of less than 0.001 compared with the corresponding value of the naive Huh7 cells. (b) Stable colony formation assay. The HCV replicon, pRep-BSD, was transfected into naive Huh7, Huh7/shRNA-HCV and Huh7/shRNA-Control cells. The cells were cultured in the presence of blasticidin S (BSD) in the medium for ~ 3 weeks, and the BSD-resistant colonies were counted. These assays were repeated twice. The colony-forming units per microgram RNA (CFU/ μ g RNA) are shown at the bottom.

(Fig. 4d). These results indicated that the decrease in luciferase activities was due to specific suppressive effects of shRNA on expression of HCV genomic RNA and the viral proteins, and not due to non-specific effects caused by the delivery of shRNA or to toxicity of the adenovirus vectors.

Absence of interferon-stimulated gene responses by siRNA delivery

It has been reported that double-stranded RNA may induce interferon-stimulated gene (ISG) responses which cause instability of mRNA, translational suppression of proteins and apoptotic cell



death.^{18,30,31} Therefore, we examined the effects of the shRNA-expressing plasmids and adenoviruses on the activation of ISG expression in cells. The ISRE-reporter plasmid, pISRE-TA-Luc, and a control plasmid, peGFPneo, were transfected into Huh7 cells

with plasmid pUC19-shRNA-HCV or pUC19-shRNA-Control, or adenovirus, AxshRNA-HCV or AxshRNA-Control, and the ISRE-mediated luciferase activities were measured. On day 2, the ISRE-luciferase activities did not significantly change in cells in which

Figure 4 Effect of a recombinant adenovirus expressing shRNA on HCV replicon. (a) Huh7/pRep-Feo cells were infected with AxshRNA-HCV or shRNA-Control at a multiplicity of infection (MOI) of 1. The cells were harvested, and internal luciferase activities were measured on day 0 through day 9 after adenovirus infection. Each assay was done in triplicate, and the value is displayed as a percentage of no treatment and as mean \pm SD. An asterisk indicates a *P*-value of less than 0.05. (b) Dimethylthiazol carboxymethoxyphenyl sulfophenyl tetrazolium (MTS) assay of Huh7/pRep-Feo cells. Cells were infected with indicated recombinant adenoviruses at an MOI of 1. The assay was done at day 6 of infection. Error bars indicate mean \pm SD. (c) Northern blotting. The upper panel shows replicon RNA, and the lower panel shows beta-actin mRNA. (d) Western blotting. Total cell lysates were separated on NuPAGE gel, blotted and incubated with monoclonal anti-NS4A or anti-NS5A antibodies. The membrane was re-blotted with antibeta-actin antibodies. NT, untreated Huh7/pRep-Feo cells; Control, cells infected with AxshRNA-Control; HCV, cells treated with AxshRNA-HCV. In panels (b) and (c), cells were harvested on day 6 after adenovirus infection at an MOI of 1.

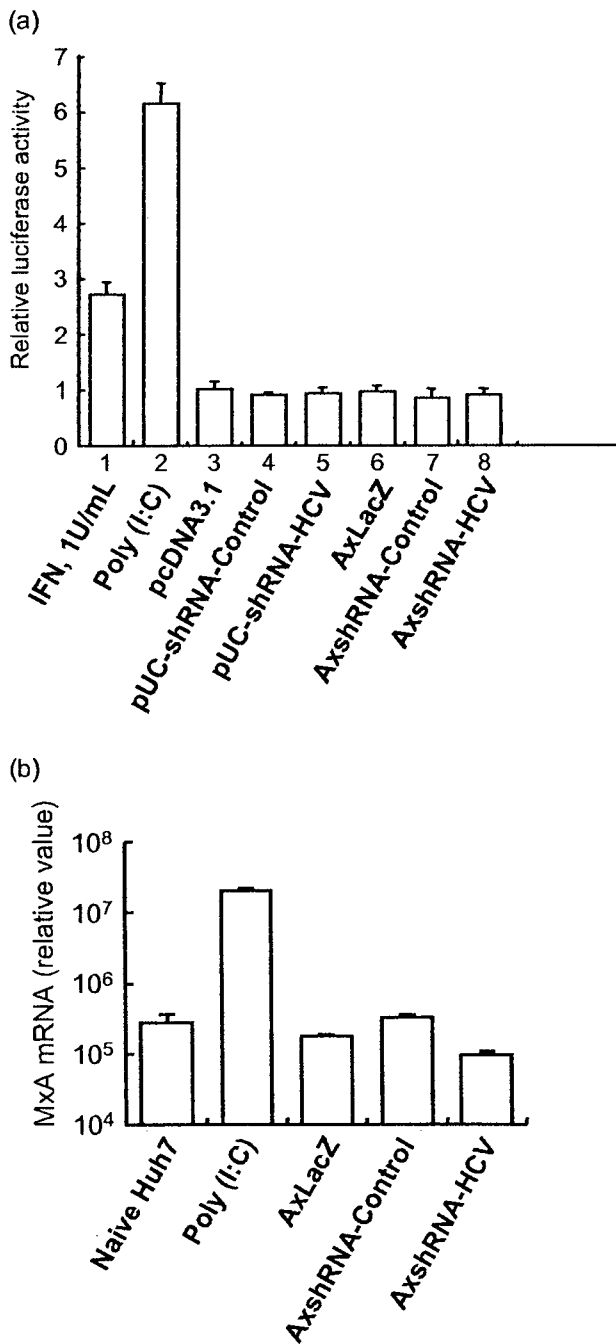


Figure 5 Interferon-stimulated gene responses by transfection of siRNA vectors. (a) Huh7 cells were seeded at 5×10^4 per well in 24-well plates on the day before transfection. As a positive control, 200 ng of pISRE-TA-Luc, or pTA-Luc, 1 ng of pRL-CMV, were transfected into a well using FuGENE-6 Transfection Reagent (Roche), and the cells were cultured with 1 U/mL of interferon (IFN) in the medium (lane 1). Lanes 3–5: 200 ng of pISRE-TA-Luc or pTA-Luc, and 1 ng of pRL-CMV were cotransfected with (lane 2) 300 ng of poly (I : C), or 200 ng of plasmids (lane 3) pcDNA3.1, (lane 4) pUC19-shRNA-Control or (lane 5) pUC19-shRNA-HCV. Lanes 6–8: 200 ng of pISRE-TA-Luc or pTA-Luc, and 1 ng of pRL-CMV were transfected, and MOI = 1 of adenoviruses, (lane 6) AxLacZ, which expressed the beta-galactosidase (LacZ) gene under control of the chicken beta-actin (CAG) promoter as a control, (lane 7) AxshRNA-Control or (lane 8) AxshRNA-HCV were infected. Dual luciferase assays were performed at 48 h after transfection. The Fluc activity of each sample was normalized by the respective Rluc activity, and the respective pTA luciferase activity was subtracted from the pISRE luciferase activity. The experiment was done in triplicate, and the data are displayed as means \pm SD. (b) Huh7 cells were infected with indicated recombinant adenoviruses, AxLacZ, AxshRNA-Control and AxshRNA-HCV. RNA was extracted from each sample at day 6, and mRNA expression levels of an interferon-inducible MxA protein were quantified by the real-time RT-PCR analysis. Primers used were as follows: human MxA sense, 5'-CGA GGG AGA CAG GAC CAT CG-3'; human MxA antisense, 5'-TCT ATC AGG AAG AAC ATT TT-3'; human beta-actin sense, 5'-ACA ATG AAG ATC AAG ATC ATT GCT CCT CCT-3'; and human beta-actin antisense, 5'-TTT GCG GTG GAC GAT GGA GGG GCC GGA CTC-3'.

negative- or positive-control shRNA plasmids was transfected. (Fig. 5a). Similarly, the expression levels of an interferon-inducible MxA protein did not significantly change by transfection of shRNA-expression vectors (Fig. 5b). These results demonstrate that the shRNA used in the present study lack induction of the ISG responses both in the form of the expression plasmids and the adenovirus vectors.

Effect of siRNA and shRNA adenoviruses on HCV-JFH1 cell culture

The effects of HCV-targeted siRNA- and shRNA-expressing adenoviruses were confirmed by using HCV-JFH1 virus cell culture system. Transfection of the siRNA #331¹⁴ into HCV-infected Huh7.5.1 cells resulted in substantial decrease of intracellular HCV RNA, while a control siRNA showed no effect (Fig. 6a). Similarly, infection of AxshRNA-HCV into Huh7.5.1/HCV-JFH1 cells specifically suppressed expression of HCV RNA (Fig. 6b).

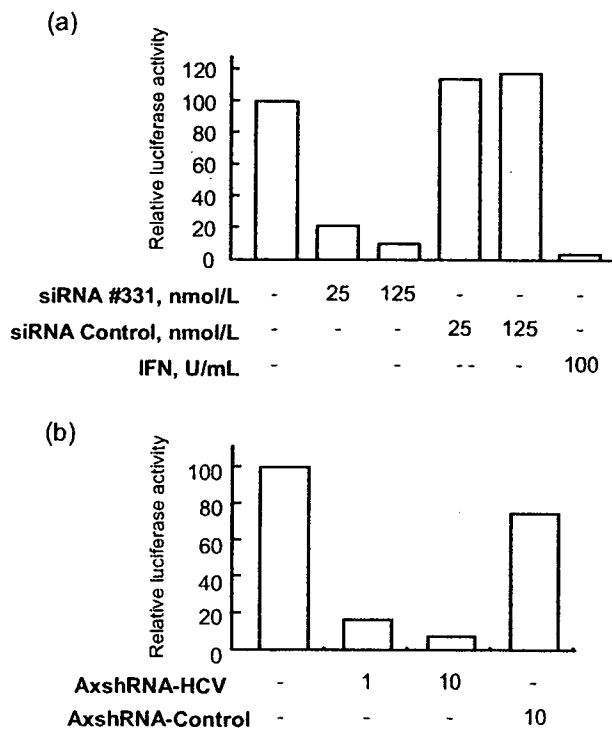


Figure 6 Effects of an siRNA and adenovirus expressing shRNA on HCV-JFH1 cell culture. (a) The siRNA #331, the siRNA-Control¹⁴, (b) AxshRNA-HCV or AxshRNA-Control were, respectively, transfected or infected onto HV-JFH1-infected Huh7.5.1 cells. Seventy-two hours of the transfection or infection, expression level of HCV-RNA was quantified by real-time RT-PCR. The assays were repeated twice, and consistent results were obtained. IFN, recombinant interferon-alpha 2b.

Suppression of HCV-IRES-mediated translation *in vivo* by adenovirus expressing shRNA

The effects of the shRNA expression on the expression of the viral structural proteins *in vivo* were investigated using conditional HCV cDNA-transgenic mice, CN2-29.²⁸ Adenoviruses, AxshRNA-HCV, AxshRNA-Control or AxCAw1 were injected into CN2-29 mice in combination with AxCANCre, an adenovirus expressing *Cre* DNA recombinase. The mice were killed on the fourth day after the injection, and the hepatic expression of the HCV core protein was measured. The expressed amounts of the core protein were 143.0 ± 56.2 pg/mg and 108.5 ± 42.4 pg/mg in AxCAw1 and AxshRNA-Control-infected mice, respectively, and the expressed amount was significantly lower in mice injected with AxshRNA-HCV (28.7 ± 7.0 pg/mg, $P < 0.05$, Fig. 7a). Similarly, the induced expression of HCV core protein was not detectable by immunohistochemistry in AxshRNA-HCV infected liver tissue (Fig. 7c). Staining of a host cellular protein, albumin, was not obviously different between the liver infected with AxCAw1, AxshRNA-HCV and AxshRNA-Control (Fig. 7d). The expression levels of two ISG, IFN-beta and Mx1, in the liver tissue were not significantly different between individuals with

and without injection of the adenovirus vectors (Fig. 7b). These results indicate specific shRNA silencing of HCV structural protein expression in the liver.

Discussion

The requirements to achieve a high efficiency using RNAi are: (i) selection of target sequences that are the most susceptible to RNAi; (ii) persistence of siRNA activity; and (iii) efficient *in vivo* delivery of siRNA to cells. We have used an shRNA sequence that was derived from a highly efficient siRNA (siRNA331), and constructed a DNA-based shRNA expression cassette that showed competitive effects with the synthetic siRNA (Fig. 2).¹⁴ The shRNA-expression cassette does not only allow extended half-life of the RNAi, but also enables use of gene-delivery vectors, such as virus vectors. As shown in the results, a retrovirus vector expressing shRNA-HCV could stably transduce cells to express HCV-directed shRNA, and the cells acquired protection against HCV subgenomic replication (Fig. 3). An adenovirus vector expressing shRNA-HCV resulted in suppression of HCV subgenomic and protein expression by around three logs to almost background levels (Fig. 4). Consistent results were obtained by using an HCV cell culture (Fig. 6). More importantly, we have demonstrated *in-vivo* effects on viral protein expression in the liver using a conditional transgenic mouse model (Fig. 7). These results suggest that efficient delivery of siRNA could be effective against HCV infection *in vivo*.

An obstacle to applying siRNA technology to treat virus infections is that viruses are prone to mutate during their replication.³² HCV continuously produces mutated viral strains to escape immune defense mechanisms. Even in a single patient, the circulating HCV population comprises a large number of closely related HCV sequence variants called quasispecies. Therefore, siRNA targeting the protein-coding sequence of the HCV genome, which have been reported by others,¹⁵⁻¹⁹ may vary considerably among different HCV genotypes, and even among strains of the same genotype.³³ Our shRNA sequence targeted the 5'-UTR of HCV RNA, which is the most conserved region among various HCV isolates.³³ In addition, the structural constraints on the 5'-UTR, in terms of its requirement to direct internal ribosome entry and translation of viral proteins, might not permit the evolution of escape mutations. Our preliminary results have shown that the siRNA-HCV suppressed replication of an HCV genotype 2a replicon³⁴ to the same extent as the HCV 1b replicon.

Although the siRNA techniques rely on a high degree of specificity, several studies report siRNA-induced non-specific effect that may result from induction of ISG responses.^{18,31} These effects may be mediated by activation of double-strand RNA-dependent protein kinase, toll-like receptor 3,³⁵ or possibly by a recently identified RNA helicase, RIG-I.³⁶ It remains to be determined whether these effects are generally induced by every siRNA construct. Sledz *et al.* have reported that transfection of two siRNA induced cellular interferon responses,³⁷ while Bridge *et al.* report that shRNA-expressing plasmids induced an interferon response but transfection of synthetic siRNA did not.³¹ Speculatively, these effects on the interferon system might be construct dependent. Our shRNA-expression plasmids and adenoviruses did not activate ISG responses *in vitro* (Fig. 5a,b) or *in vivo* (Fig. 7b). We have preliminarily detected phosphorylated PKR (P-PKR) by western

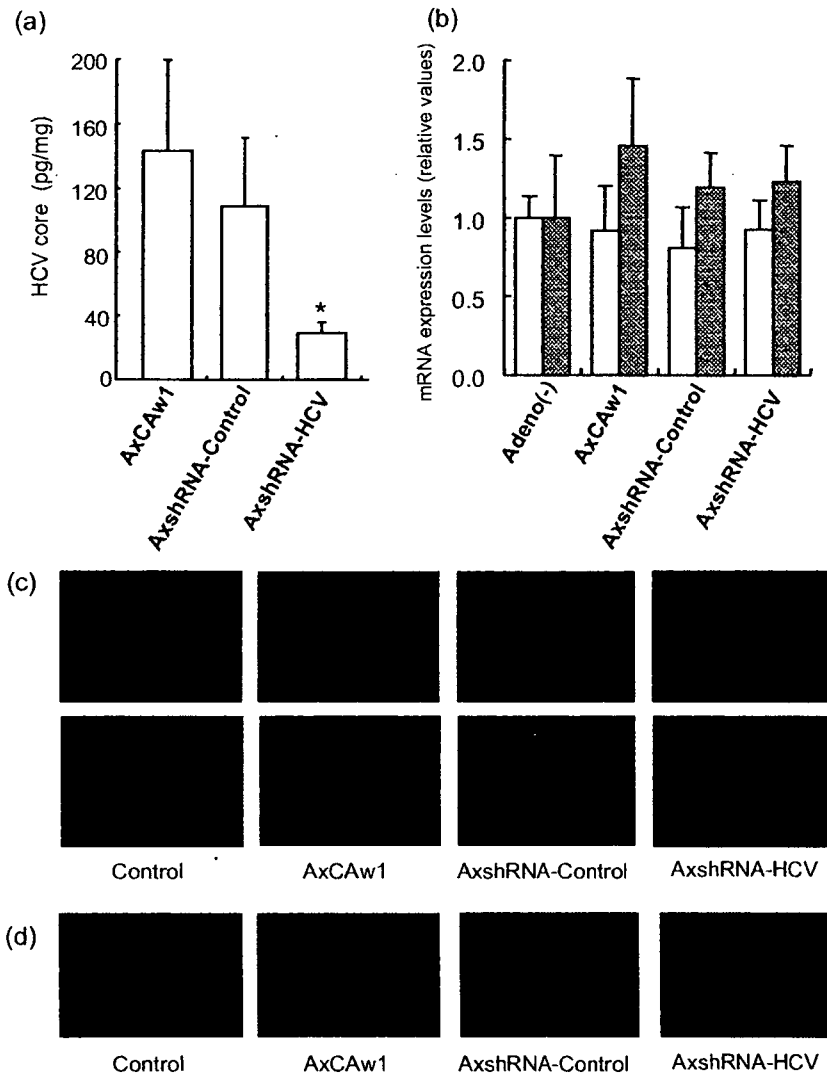


Figure 7 Effects of a recombinant adenovirus expressing shRNA on HCV core protein expression in CN2-29 transgenic mice. CN2-29 transgenic mice were administered with 1×10^9 PFU of AxCANCre combined with 6.7×10^8 PFU of AxshRNA-HCV, AxshRNA or AxCAw1. The mice were killed on day 4 after injection. (a) Quantification of HCV core protein in liver. Liver tissues were homogenized and used to determine the amount of HCV core protein. Each assay was done in triplicate, and the values are displayed as mean \pm SD. Asterisk indicates *P*-value of less than 0.05. (b) Expression levels of mouse interferon-beta (white bars) and Mx1 (shaded bars) mRNA in the mouse liver tissue were quantified by the real-time RT-PCR analyses. Primers used were as follows: mouse interferon-beta sense, 5'-ACA GCC CTC TCC ATC AAC TA-3'; mouse interferon-beta antisense, 5'-CCC TCC AGT AAT AGC TCT TC-3'; mouse Mx1 sense, 5'-AGG AGT GGA GAG GCA AAG TC-3'; mouse Mx1 antisense, 5'-CAC ATT GCT GGG GAC TAC CA-3'; mouse beta-actin sense, 5'-ACT CCT ATG TGG GTG ACG AG-3'; mouse beta-actin antisense, 5'-ATA GCC CTC GTA GAT GGG CA-3'. Adeno (-) denotes mice without adenovirus administration. (c) Immunofluorescence microscopy of HCV core protein in the liver tissue. Liver sections of mice were stained using rabbit anticore polyclonal antibody and normal rabbit IgG as a negative control. The upper photographs were obtained at 400x magnification, and the lower photographs were at 1000x. (d) Immunofluorescence microscopy of albumin in liver. Liver sections from the mice were fixed and stained using rabbit antialbumin antibody and normal rabbit IgG as a negative control.

blotting, and found no apparent increase of P-PKR (data not shown). These results indicate that these target sequences and structures are of sufficient specificity to silence the target gene without eliciting non-specific interferon responses.

Beside the canonical action of siRNA, a sequence-specific cleavage of target mRNA, the siRNA could act as a micro-RNA

that suppresses translational initiation of mRNA,³⁸ or it could mediate transcriptional gene silencing.³⁹ Regarding our *in-vivo* experiments, it was difficult to differentially analyze the effect of siRNA at individual sites of action because post-translational effect of siRNA concomitantly destabilizes target mRNA, which leads to apparent decrease of mRNA transcripts.

Efficiency and safety of gene transfer methods are the key determinants of the clinical success of gene therapy and an unresolved problem. There are several reports of delivery of siRNA or siRNA-expression vectors to cells *in vivo*;^{12,40,41} however, gene delivery methods that are safe enough to apply to clinical therapeutics are currently under development. Adenovirus vectors are one of the most commonly used carriers for human gene therapies.^{42–44} Our present results demonstrate that the adenoviral delivery of shRNA is effective in blocking HCV replication *in vitro* and virus protein expression *in vivo*. Adenovirus vectors have several advantages of efficient delivery of transgene both *in vitro* and *in vivo* and natural hepatotropism when administered *in vivo*. The AxshRNA-HCV specifically blocked expression of HCV structural proteins in a conditional transgenic mouse expressing those proteins. The current adenovirus vectors may cause inflammatory reactions in the target organ,⁴⁵ however, and produce neutralizing antibodies which make repeated administration difficult. These problems may be overcome by the improved constructs of virus vectors with attenuated immunogenicity or by the development of non-viral carriers for gene delivery.⁴⁶

In conclusion, our results demonstrate the effectiveness and feasibility of the siRNA expression system. The efficiency of adenovirus expressing shRNA that target HCV suggests that delivery and expression of siRNA in hepatocytes may eliminate the virus and that this RNA-targeting approach might provide a potentially effective future therapeutic option for HCV infection.

Acknowledgments

This study was supported by grants from Japan Society for the Promotion of Science, 15590629 and 16590580, and partly supported by a grant from the Viral Hepatitis Research Foundation of Japan.

References

- Alter MJ. Epidemiology of hepatitis C. *Hepatology* 1997; **26**: 62S–65S.
- Hadziyannis SJ, Sette H Jr, Morgan TR *et al.* Peginterferon-alpha2a and ribavirin combination therapy in chronic hepatitis C: a randomized study of treatment duration and ribavirin dose. *Ann. Intern. Med.* 2004; **140**: 346–55.
- Fire A, Xu S, Montgomery M, Kostas S, Driver S, Mello C. Potent and specific genetic interference by double-stranded RNA in *Caenorhabditis elegans*. *Nature* 1998; **391**: 806–11.
- Elbashir SM, Harborth J, Lendeckel W, Yalcin A, Weber K, Tuschl T. Duplexes of 21-nucleotide RNAs mediate RNA interference in cultured mammalian cells. *Nature* 2001; **411**: 494–8.
- Coburn GA, Cullen BR. Potent and specific inhibition of human immunodeficiency virus type 1 replication by RNA interference. *J. Virol.* 2002; **76**: 9225–31.
- Jacque JM, Triques K, Stevenson M. Modulation of HIV-1 replication by RNA interference. *Nature* 2002; **418**: 435–8.
- Gitlin L, Karelsky S, Andino R. Short interfering RNA confers intracellular antiviral immunity in human cells. *Nature* 2002; **418**: 430–4.
- Ge Q, Filip L, Bai A, Nguyen T, Eisen HN, Chen J. Inhibition of influenza virus production in virus-infected mice by RNA interference. *Proc. Natl. Acad. Sci. USA* 2004; **101**: 8676–81.
- Wang C, Pflugheber J, Sumpter R Jr *et al.* Alpha interferon induces distinct translational control programs to suppress hepatitis C virus RNA replication. *J. Virol.* 2003; **77**: 3898–912.
- Klein C, Bock CT, Wedemeyer H *et al.* Inhibition of hepatitis B virus replication *in vivo* by nucleoside analogues and siRNA. *Gastroenterology* 2003; **125**: 9–18.
- Konishi M, Wu CH, Wu GY. Inhibition of HBV replication by siRNA in a stable HBV-producing cell line. *Hepatology* 2003; **38**: 842–50.
- McCaffrey AP, Meuse L, Pham TT, Conklin DS, Hannon GJ, Kay MA. RNA interference in adult mice. *Nature* 2002; **418**: 38–9.
- Shlomai A, Shaul Y. Inhibition of hepatitis B virus expression and replication by RNA interference. *Hepatology* 2003; **37**: 764–70.
- Yokota T, Sakamoto N, Enomoto N *et al.* Inhibition of intracellular hepatitis C virus replication by synthetic and vector-derived small interfering RNAs. *EMBO Rep.* 2003; **4**: 602–8.
- Kapadia SB, Brideau-Andersen A, Chisari FV. Interference of hepatitis C virus RNA replication by short interfering RNAs. *Proc. Natl. Acad. Sci. USA* 2003; **100**: 2014–18.
- Kronke J, Kittler R, Buchholz F *et al.* Alternative approaches for efficient inhibition of hepatitis C virus RNA replication by small interfering RNAs. *J. Virol.* 2004; **78**: 3436–46.
- Randall G, Grakoui A, Rice CM. Clearance of replicating hepatitis C virus replicon RNAs in cell culture by small interfering RNAs. *Proc. Natl. Acad. Sci. USA* 2003; **100**: 235–40.
- Seo MY, Abrignani S, Houghton M, Han JH. Letter to the editor: small interfering RNA-mediated inhibition of hepatitis C virus replication in the human hepatoma cell line Huh-7. *J. Virol.* 2003; **77**: 810–12.
- Wilson JA, Jayasena S, Khvorova A *et al.* RNA interference blocks gene expression and RNA synthesis from hepatitis C replicons propagated in human liver cells. *Proc. Natl. Acad. Sci. USA* 2003; **100**: 2783–8.
- Guo JT, Bichko VV, Seeger C. Effect of alpha interferon on the hepatitis C virus replicon. *J. Virol.* 2001; **75**: 8516–23.
- Tanabe Y, Sakamoto N, Enomoto N *et al.* Synergistic inhibition of intracellular hepatitis C virus replication by combination of ribavirin and interferon-alpha. *J. Infect. Dis.* 2004; **189**: 1129–39.
- Maekawa S, Enomoto N, Sakamoto N *et al.* Introduction of NS5A mutations enables subgenomic HCV-replicon derived from chimpanzee-infectious HC-J4 isolate to replicate efficiently in Huh-7 cells. *J. Viral. Hepat.* 2004; **11**: 394–403.
- Miyagishi M, Sumimoto H, Miyoshi H, Kawakami Y, Taira K. Optimization of an siRNA-expression system with an improved hairpin and its significant suppressive effects in mammalian cells. *J. Gene Med.* 2004; **6**: 715–23.
- Li Y, Yokota T, Matsunura R, Taira K, Mizusawa H. Sequence-dependent and independent inhibition specific for mutant ataxin-3 by small interfering RNA. *Ann. Neurol.* 2004; **56**: 124–9.
- Kanazawa N, Kurosaki M, Sakamoto N *et al.* Regulation of hepatitis C virus replication by interferon regulatory factor-1. *J. Virol.* 2004; **78**: 9713–20.
- Wakita T, Pietschmann T, Kato T *et al.* Production of infectious hepatitis C virus in tissue culture from a cloned viral genome. *Nat. Med.* 2005; **11**: 791–6.
- Zhong J, Gastaminza P, Cheng G *et al.* Robust hepatitis C virus infection *in vitro*. *Proc. Natl. Acad. Sci. USA* 2005; **102**: 9294–9.
- Wakita T, Taya C, Katsume A *et al.* Efficient conditional transgene expression in hepatitis C virus cDNA transgenic mice mediated by the Cre/loxP system. *J. Biol. Chem.* 1998; **273**: 9001–6.
- Kashiwakuma T, Hasegawa A, Kajita T *et al.* Detection of hepatitis C virus specific core protein in serum of patients by a sensitive fluorescence enzyme immunoassay (FEIA). *J. Immunol. Methods* 1996; **28**: 79–89.

- 30 Baglioni C, Nilsen TW. Mechanisms of antiviral action of interferon. *Interferon* 1983; **5**: 23–42.
- 31 Bridge A, Pebernard S, Ducraux A, Nicoulaz A, Iggo R. Induction of an interferon response by RNAi vectors in mammalian cells. *Nat. Genet.* 2003; **34**: 263–4.
- 32 Carmichael GG. Silencing viruses with RNA. *Nature* 2002; **418**: 379–80.
- 33 Okamoto H, Okada S, Sugiyama Y *et al.* Nucleotide sequence of the genomic RNA of hepatitis C virus isolated from a human carrier: comparison with reported isolates for conserved and divergent regions. *J. Gen. Virol.* 1991; **72**: 2697–704.
- 34 Kato T, Date T, Miyamoto M *et al.* Efficient replication of the genotype 2a hepatitis C virus subgenomic replicon. *Gastroenterology* 2003; **125**: 1808–17.
- 35 Alexopoulou L, Holt AC, Medzhitov R, Flavell RA. Recognition of double-stranded RNA and activation of NF- κ B by Toll-like receptor 3. *Nature* 2001; **413**: 732–8.
- 36 Yoneyama M, Kikuchi M, Natsukawa T *et al.* The RNA helicase RIG-I has an essential function in double-stranded RNA-induced innate antiviral responses. *Nat. Immunol.* 2004; **5**: 730–7.
- 37 Sledz C, Holko M, de Veer M, Silverman R, Williams, B. Activation of the interferon system by short-interfering RNAs. *Nat. Cell. Biol.* 2003; **5**: 834–9.
- 38 Doench JG, Petersen CP, Sharp PA. siRNAs can function as miRNAs. *Genes Dev.* 2003; **17**: 438–42.
- 39 Morris KV. siRNA-mediated transcriptional gene silencing: the potential mechanism and a possible role in the histone code. *Cell. Mol. Life Sci.* 2005; **62**: 3057–66.
- 40 Xia H, Mao Q, Paulson HL, Davidson BL. siRNA-mediated gene silencing in vitro and in vivo. *Nat. Biotechnol.* 2002; **20**: 1006–10.
- 41 Zender L, Hutker S, Liedtke C *et al.* Caspase 8 small interfering RNA prevents acute liver failure in mice. *Proc. Natl. Acad. Sci. USA* 2003; **100**: 7797–802.
- 42 Akli S, Caillaud C, Vigne E *et al.* Transfer of a foreign gene into the brain using adenovirus vectors. *Nat. Genet.* 1993; **3**: 224–8.
- 43 Bajocchi G, Feldman SH, Crystal RG, Mastrangeli A. Direct in vivo gene transfer to ependymal cells in the central nervous system using recombinant adenovirus vectors. *Nat. Genet.* 1993; **3**: 229–34.
- 44 Davidson BL, Allen ED, Kozarsky KF, Wilson JM, Roesler BJ. A model system for in vivo gene transfer into the central nervous system using an adenoviral vector. *Nat. Genet.* 1993; **3**: 219–23.
- 45 Yang Y, Wilson JM. Clearance of adenovirus-infected hepatocytes by MHC class I-restricted CD4+ CTLs in vivo. *J. Immunol.* 1995; **155**: 2564–70.
- 46 Fleury S, Driscoll R, Simeoni E *et al.* Helper-dependent adenovirus vectors devoid of all viral genes cause less myocardial inflammation compared with first-generation adenovirus vectors. *Basic Res. Cardiol.* 2004; **99**: 247–56.

Identification of Novel Epoxide Inhibitors of Hepatitis C Virus Replication Using a High-Throughput Screen^{†‡§}

Lee F. Peng,^{1,2,3,‡} Sun Suk Kim,^{1,4,‡} Sirinya Matchacheep,^{2,3} Xiaoguang Lei,⁵ Shun Su,⁵ Wenyu Lin,¹ Weerawat Runguphan,^{2,3} Won-Hyeok Choe,¹ Naoya Sakamoto,⁶ Masanori Ikeda,⁷ Nobuyuki Kato,⁷ Aaron B. Beeler,⁵ John A. Porco, Jr.,⁵ Stuart L. Schreiber,^{2,3,8} and Raymond T. Chung^{1*}

GI Unit, Department of Medicine, Massachusetts General Hospital, 55 Fruit Street, Boston, Massachusetts 02114¹; Department of Chemistry and Chemical Biology, Harvard University, 12 Oxford Street, Cambridge, Massachusetts 02138²; The Broad Institute of Harvard and MIT, 7 Cambridge Center, Cambridge, Massachusetts 02142³; Department of Gastroenterology and Hepatology, Gachon University Gil Medical Center, 1198 Guwol-dong, Namdong-gu, Incheon, 405-760 Korea⁴; Department of Chemistry and Center for Chemical Methodology and Library Development (CMLD-BU), Boston University, 590 Commonwealth Avenue, Boston, Massachusetts 02215⁵; Department of Gastroenterology and Hepatology, Tokyo Medical and Dental University, Tokyo, Japan⁶; Department of Molecular Biology, Okayama University Graduate School of Medicine, Dentistry, and Pharmaceutical Sciences, Okayama, Japan⁷; and Howard Hughes Medical Institute, Chevy Chase, Maryland⁸

Received 15 February 2007/Returned for modification 7 May 2007/Accepted 28 July 2007

Using our high-throughput hepatitis C replicon assay to screen a library of over 8,000 novel diversity-oriented synthesis (DOS) compounds, we identified several novel compounds that regulate hepatitis C virus (HCV) replication, including two libraries of epoxides that inhibit HCV replication (best 50% effective concentration, < 0.5 μ M). We then synthesized an analog of these compounds with optimized activity.

Hepatitis C virus (HCV) infects over 170 million people worldwide and frequently leads to cirrhosis, liver failure, and hepatocellular carcinoma (1). Currently, the best therapy for the treatment of chronic hepatitis C is a combination of pegylated interferon and ribavirin, which has suboptimal efficacy and has an unfavorable side effect profile (14). The identification of more-effective and better-tolerated agents is therefore a high priority.

We have recently reported the successful adaptation of the Huh7/Rep-Feo replicon cell line (18) to a high-throughput screening assay system (8). Using this system, we previously screened a library of 2,568 well-known compounds whose biological activity is fully characterized (8). In order to discover novel regulators of HCV replication, we then screened a library of 8,064 diversity-oriented synthesis (DOS) compounds (15, 16). This library, known as the DOS set, is a

TABLE 1. Hits by library from the primary high-throughput screening with the DOS set^a

Library	Increased luciferase signal hit libraries			Antiviral hit libraries		
	Hits	Members	Reference(s)	Hits	Members	Reference(s) or sources
FPA	11	319	5			
BUCMLD	4	880	10, 17	4	880	10, 17, Fig. 1, Table 2
JMM	4	544	13			
UGISS	1	319	2			
BUCMLD epoxyquinol				12	34	10, 17, Fig. 1 and 2, Table 2
SM				9	27	Fig. 1 and 2, Table 2
SpOx				6	612	6, 12
BEA				3	238	3
ICCB6				3	352	4
YKK				2	281	9
RTE				2	159	19

^a The total number of compounds which comprise each library is listed in the "Members" columns.

* Corresponding author. Mailing address: GRJ 825A, GI Unit, Massachusetts General Hospital, Boston, MA 02114. Phone: (617) 724-7562. Fax: (617) 726-5895. E-mail: rtchung@partners.org.

† This publication is dedicated to Yoshito Kishi on the occasion of his 70th birthday.

§ Supplemental material for this article may be found at <http://aac.asm.org/>.

‡ L.F.P. and S.S.K. contributed equally to this project.

¶ Published ahead of print on 6 August 2007.

TABLE 2. Results of secondary screening with antiviral hit compounds from the SM and BUCMLD libraries^a

Compound name	EC ₅₀	CC ₅₀
BUCMLD-B10A11	<0.5 (<0.5–0.5)	19.5 (19.4–22.4)
BUCMLD-B10A3	0.7 (<0.5–5.2)	9.0 (7.1–10.0)
BUCMLD-XL-184	1.4 (0.8–3.9)	>50
BUCMLD-B10A5	1.5 (<0.5–5.4)	39.3 (28.6–>50)
BUCMLD-XL-190	2.5 (<0.5–10)	>50
BUCMLD-B10A1	2.6 (1.0–5.0)	18.0 (15.9–19.5)
SM_A14B5	3.5 (2.7–4.4)	27.1 (18.0–44.6)
BUCMLD-XL-189	3.8 (2.2–7.0)	>50
SM_A6B5_2P100	6.6 (4.0–15.3)	>50
BUCMLD-B10A8	7.0 (0.9–30.0)	>50
BUCMLD-B10A10	7.0 (5.4–30.0)	>50
BUCMLD-B10A14	7.6 (1.0–23.0)	>50
BUCMLD-B10A7	7.75 (1.0–30.0)	35.3 (33.6–36.7)
SM_A4B6_2P123	8.0 (6.3–10.0)	>50
SM_A5B5_2P118	9.1 (2.5–16.7)	>50
SM_A7C2_2P155	12.7 (7.0–24.0)	>50
BUCMLD-B13A2	14.2 (6.4–45.0)	>50
SM_A1B2_1P32	19.6 (11.7–28.2)	>50
SM_A1B5_2P24	19.7 (6.25–50.0)	>50
BUCMLD-B13A1	21.1 (7.5–36.7)	>50
SM_A5B3_2P141	25.7 (18.3–39.8)	>50
SM_A5B2_2P142	26.7 (9.1–50.0)	>50
BUCMLD-NTM-EN2-67A	30.0 (0.7–46.1)	>50
SM_A12B3	>30	>50
BUCMLD-B10A13	42.9 (25.2–59.4)	>50
BUCMLD-XL-130	>100	>50

^a Note that structure-activity relationship SM library compounds are also included. The EC₅₀ and 50% cytotoxic concentration (CC₅₀) are reported in μM with 95% confidence intervals in parentheses. A value of <0.5 indicates a concentration of less than 0.5 μM ; >30 indicates a concentration of greater than 30 μM ; >50 indicates a concentration of greater than 50 μM ; and >100 indicates a concentration of greater than 100 μM .

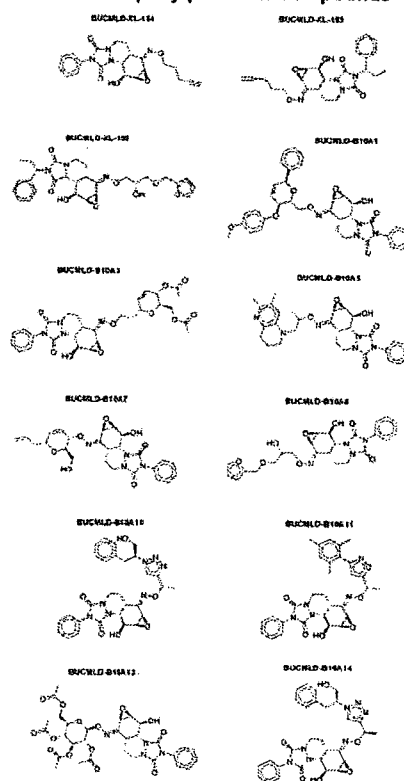
meta-library comprised of DOS libraries from chemists throughout the United States and Canada. Information about the DOS set is available at http://www.broad.harvard.edu/chembio/platform/screening/compound_libraries/index.htm.

The high-throughput primary screen and the secondary validation assays were performed as described in our previous publication (8).

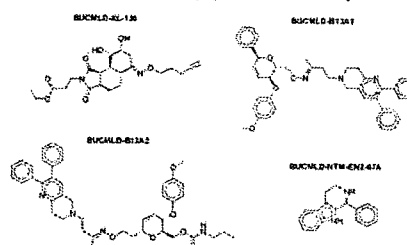
Computational data analysis of the primary screening results was performed as previously described (8) except for the hit criteria. As the characteristics of this data set are different from those generated by our previous screen (8), different threshold values were chosen to assure optimal hit selection. Compounds were considered hits for inhibiting replication if they had a composite Z score of <−2.57 in the reporter gene screen, a reproducibility of >0.9 or <−0.9 in that screen, and a composite Z score of >−2.00 in the cell viability screen. Compounds were considered hits for stimulating luciferase production if they had a composite Z score of >2.50 in the reporter gene screen, a reproducibility of >0.9 or <−0.9 in that screen, and a composite Z score of <1.00 in the cell viability screen.

Full synthetic experimental procedures and spectroscopic data for the SM library compounds discussed in this publication are provided in the supplemental material. The synthesis of the full SM library, including compounds not discussed here, will be the subject of an upcoming report.

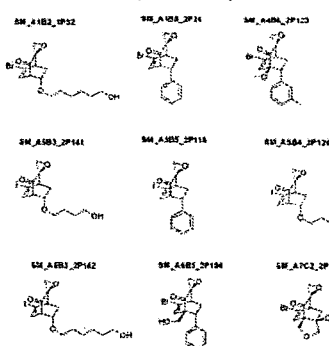
BUCMLD Epoxyquinol Hit Compounds



BUCMLD Non-Epoxyquinol Hit Compounds



SM Library Hit Compounds



SM Library SAR Compounds

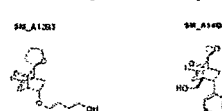


FIG. 1. Structures of antiviral hit compounds from the BUCMLD and SM libraries. SAR, structure-activity relationship.

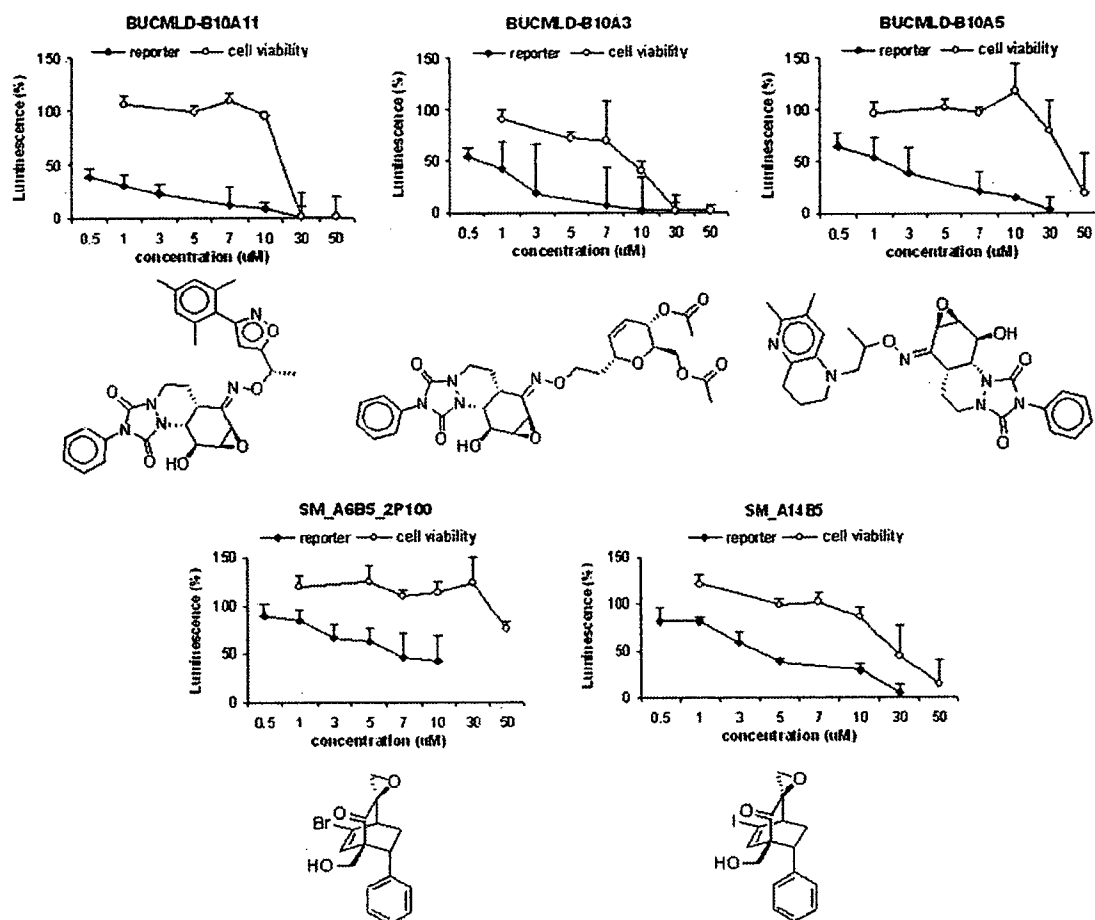


FIG. 2. Selected graphical results of secondary screening with antiviral hit compounds from the SM and BUCMLD epoxyquinol libraries. Luciferase activity for HCV RNA replication levels is shown as a percentage of control. Cell viability is also shown as a percentage of control. Each point represents the average of triplicate data points with standard deviation represented as the error bar.

The synthesis of the BUCMLD epoxyquinol library has been previously described (10, 17).

Full experimental details regarding the JFH1 HCVcc system (11) are provided in the supplemental material. We identified 41 antiviral compounds that inhibited HCV replication and 20 proviral compounds that increased luciferase production (Table 1). In our analysis of the antiviral hit compounds from the DOS set, a striking finding was that 21 of the 41 compounds contained an epoxide moiety. Moreover, the most potent of these compounds were epoxides. Further analysis revealed that these epoxides came from only two DOS libraries, SM and BUCMLD epoxyquinol (10, 17), with very high sublibrary hit rates of 35% and 33%, respectively (Table 1). Of note, the non-hit members of these two libraries did exhibit antiviral activity but failed to meet the formal hit criteria.

As we were especially intrigued by these epoxide-bearing compounds, we restricted our hit validation to these compounds (Table 2 and Fig. 1). SM_A6B5_2P100 was the most active member of the SM library, while BUCMLD-B10A11 was the most potent member of the BUCMLD epoxyquinol library (Table 2 and Fig. 2).

Structure-activity relationship analysis of the SM library reveals the structural elements most important for antiviral

activity (Table 2 and Fig. 1). Comparing SM_A5B5_2P118 to SM_A1B5_2P24, iodinated compounds are more active than brominated ones. Comparing SM_A5B5_2P118 to SM_A5B3_2P141 and SM_A5B2_2P142, compounds with a phenyl substituent are more active than those with aliphatic chains. Finally, the most active compounds, SM_A4B6_2P123 and SM_A6B5_2P100, have a bridgehead substituent. Thus, we hypothesized that the most active compound should bear an iodine, a phenyl substituent, and a bridgehead substituent.

SM_A14B5, which incorporates all of these elements, was therefore synthesized, as it was reasoned to be the most active SM library compound. Indeed, SM_A14B5 had a 50% effective concentration (EC_{50}) of approximately 3.5 μ M, which is about half that of SM_A6B5_2P100 (Table 2 and Fig. 2).

The most potent compounds from each library, SM_A14B5 and BUCMLD-B10A11, underwent further validation in the infectious JFH1 HCVcc system (11). They were tested at concentrations of 5 μ M and 1 μ M, respectively, and inhibited HCV replication 48.4% \pm 5.9% and 45.1% \pm 5.2%, respectively, relative to the level of inhibition achieved by interferon at a concentration of 1 ng/ml. These data roughly approximate the EC_{50} validation data derived from the OR6 system (7) in

which inhibition was also measured relative to that of interferon at a concentration of 1 ng/ml.

Our observations suggest that the epoxide moiety is essential for potent antiviral activity. Analyzing the BUCMLD compounds, those compounds that bear an epoxide moiety are, in general, more-potent antivirals than those that do not (Table 2 and Fig. 1). Furthermore, all of the compounds from the SM library bear epoxides. SM_A12B3, an analog of SM_A5B3_2P141, which bears a tetrahydrofuran moiety in place of an epoxide, was therefore synthesized to further test this hypothesis. SM_A12B3 had negligible antiviral activity (Table 2), while SM_A5B3_2P141 displayed modest antiviral activity. Other analogs of SM compounds bearing tetrahydrofuran rings in place of epoxides showed similar attenuation of antiviral activity relative to their parent compounds. Unfortunately, attempts to synthesize the tetrahydrofuran analog of the most potent SM compound, SM_A14B5, have so far been unsuccessful.

It is interesting to note that it is the urazole-containing epoxyquinol constituents of the BUCMLD epoxyquinol library, rather than the maleimide-derived ones, that demonstrated anti-HCV activity in the primary screen. It is therefore likely that the combination of a urazole with the epoxide is necessary for the activity of the BUCMLD epoxyquinol compounds.

Although none of our most potent antiviral DOS compounds showed significant cytotoxicity at their EC_{50} s, all of them ultimately proved to be cytotoxic at higher concentrations (Table 2 and Fig. 2). Therefore, future modifications should not only aim to improve anti-HCV activity but should also attempt to decrease cytotoxicity, in order to widen the therapeutic window.

It is tempting to hypothesize that these epoxides exert their antiviral effects through a common pathway. Presumably, they act as electrophiles, with the nucleophilic target making a covalent bond by attacking and opening the epoxides. Studies to elucidate their mechanism of action are under way.

We thank the National Cancer Institute and the Initiative for Chemical Genetics, who provided support for this publication, and the Chemical Biology Platform of the Broad Institute of Harvard and MIT for their assistance in this work.

The project has been funded in whole or in part with federal funds from the National Cancer Institute's Initiative for Chemical Genetics, National Institutes of Health, under contract no. N01-CO-12400.

The content of this publication does not necessarily reflect the views or policies of the Department of Health and Human Services, nor does mention of trade names, commercial products, or organizations imply endorsement by the U.S. government.

Financial support was provided by the following: The American Gastroenterological Association FDHN/TAP Pharmaceuticals FFT Award (L.F.P.), The GlaxoSmithKline Research Fund of the Korean Association for The Study of The Liver (S.S.K.), NIH 5T32DK07191-31 (L.F.P.), NIH NS050854-01 (R.T.C.), and the NIGMS CMLD Initiative P50 GM067041 (J.A.P.).

REFERENCES

- Alter, M. J. 2006. Epidemiology of hepatitis C. *Hepatology* 43:S207–S220.
- Andreana, P. R., C. C. Liu, and S. L. Schreiber. 2004. Stereochemical control of the Passerini reaction. *Org. Lett.* 6:4231–4233.
- Brittain, D. E. A., B. L. Gray, and S. L. Schreiber. 2005. From solution-phase to solid-phase enyne metathesis: crossover in the relative performance of two commonly used ruthenium pre-catalysts. *Chem. Eur. J.* 11:5086–5093.
- Burke, M. D., E. M. Berger, and S. L. Schreiber. 2004. A synthesis strategy yielding skeletally diverse small molecules combinatorially. *J. Am. Chem. Soc.* 126:14095–14104.
- Chen, C., X. Li, C. Neumann, M. M.-C. Lo, and S. L. Schreiber. 2005. Convergent diversity-oriented synthesis of small-molecule hybrids. *Angew. Chem.* 117:2–4.
- Chen, C., X. Li, and S. L. Schreiber. 2003. Catalytic asymmetric [3+2] cycloaddition of azomethine ylides. Development of a versatile stepwise, three-component reaction for diversity-oriented synthesis. *J. Am. Chem. Soc.* 125:10174–10175.
- Ikeda, M., K. Abe, H. Dansako, T. Nakamura, K. Naka, and N. Kato. 2005. Efficient replication of a full-length hepatitis C virus genome, strain O, in cell culture, and development of a luciferase reporter system. *Biochem. Biophys. Res. Commun.* 329:1350–1359.
- Kim, S. S., L. F. Peng, W. Lin, W.-H. Choe, N. Sakamoto, S. L. Schreiber, and R. T. Chung. 2007. A cell-based, high-throughput screen for small molecule regulators of HCV replication. *Gastroenterology* 132:311–320.
- Kim, Y.-K., M. A. Arai, T. Arai, J. O. Lamenzo, E. F. Dean, N. Patterson, P. A. Clemons, and S. L. Schreiber. 2004. Relationship of stereochemical and skeletal diversity of small molecules to cellular measurement space. *J. Am. Chem. Soc.* 126:14740–14745.
- Lei, X., N. Zaarur, M. Y. Sherman, and J. A. Porco. 2005. Stereocontrolled synthesis of a complex library via elaboration of angular epoxyquinol scaffolds. *J. Org. Chem.* 70:6474–6483.
- Lindenbach, B. D., M. J. Evans, A. J. Syder, B. Wolk, T. L. Tellinghuisen, C. C. Liu, T. Maruyama, R. O. Hynes, D. R. Burton, J. A. McKeating, and C. M. Rice. 2005. Complete replication of hepatitis C virus in cell culture. *Science* 309:623–626.
- Lo, M. M.-C., C. S. Neumann, S. Nagayama, E. O. Perlstein, and S. L. Schreiber. 2004. A library of spirooxindoles based on a stereoselective three-component coupling reaction. *J. Am. Chem. Soc.* 126:16077–16086.
- Mitchell, J. M., and J. T. Shaw. 2006. A structurally diverse library of polycyclic lactams resulting from systematic placement of proximal functional groups. *Angew. Chem.* 45:1722–1726.
- Pawlotsky, J. M. 1997. Therapy of hepatitis C: from empiricism to eradication. *Hepatology* 26:S62–S65.
- Schreiber, S. L. 2000. Target-oriented and diversity-oriented organic synthesis in drug discovery. *Science* 287:1964–1969.
- Schreiber, S. L. 2003. Chemical genetics. *Chem. Eng. News* 81:51–61.
- Su, S., D. E. Acquilano, J. Arumugasamy, A. B. Beeler, E. L. Eastwood, J. R. Giguere, P. Lan, X. Lei, G. K. Min, A. R. Yeager, Y. Zhou, J. S. Panek, J. K. Snyder, S. E. Schaus, and J. A. Porco. 2005. Convergent synthesis of a complex oxime library using chemical domain shuffling. *Org. Lett.* 7:2751–2754.
- Tanabe, Y., N. Sakamoto, N. Enomoto, M. Kurosaki, E. Ueda, S. Maekawa, T. Yamashiro, M. Nakagawa, C. H. Chen, N. Kanazawa, S. Kakinuma, and M. Watanabe. 2004. Synergistic inhibition of intracellular hepatitis C virus replication by combination of ribavirin and interferon. *J. Infect. Dis.* 189: 1129–1139.
- Taylor, A. M., and S. L. Schreiber. 2006. Enantioselective addition of terminal alkynes to isolated isoquinoline iminiums. *Org. Lett.* 8:143–146.



Development of plaque assays for hepatitis C virus-JFH1 strain and isolation of mutants with enhanced cytopathogenicity and replication capacity

Yuko Sekine-Osajima ^{a,1}, Naoya Sakamoto ^{a,b,*}, Kako Mishima ^a, Mina Nakagawa ^{a,b}, Yasuhiro Itsui ^a, Megumi Tasaka ^a, Yuki Nishimura-Sakurai ^a, Cheng-Hsin Chen ^a, Takanori Kanai ^a, Kiichiro Tsuchiya ^a, Takaji Wakita ^c, Nobuyuki Enomoto ^d, Mamoru Watanabe ^a

^a Department of Gastroenterology and Hepatology, Tokyo Medical and Dental University, Tokyo, Japan

^b Department for Hepatitis Control, Tokyo Medical and Dental University, Tokyo, Japan

^c Department of Virology II, National Institute of Infectious Diseases, Tokyo, Japan

^d First Department of Internal Medicine, University of Yamanashi, Yamanashi, Japan

Received 15 June 2007; returned to author for revision 10 July 2007; accepted 9 September 2007

Available online 22 October 2007

Abstract

HCV culture *in vitro* results in massive cell death, which suggests the presence of HCV-induced cytopathic effects. Therefore, we investigated its mechanisms and viral nucleotide sequences involved in this effect using HCV-JFH1 cell culture and a newly developed HCV plaque assay technique. The plaque assay developed cytopathic plaques, depending on the titer of the inoculum. In the virus-infected cells, the ER stress markers, GRP78 and phosphorylated eIF2- α , were overexpressed. Cells in the plaques were strongly positive for an apoptosis marker, annexin V. Isolated virus subclones from individual plaque showed greater replication efficiency and cytopathogenicity than the parental virus. The plaque-purified virus had 9 amino acid substitutions, of which 5 were clustered in the C terminal of the NS5B region. Taken together, the cytopathic effect of HCV infection involves ER-stress-induced apoptotic cell death. Certain HCV genomic structures may determine the viral replication capacity and cytopathogenicity.

© 2007 Elsevier Inc. All rights reserved.

Keywords: HCV-JFH1; HCV cell culture; Plaque assay; ER stress; Unfolded protein responses; Apoptosis; NS5B RNA-dependent RNA polymerase

Introduction

Molecular analyses of the HCV life cycle, virus–host interactions, and mechanisms of liver cell damage by the virus are not understood completely, mainly because of the lack of cell culture systems. These problems have been partly overcome by the development of the HCV subgenomic replicon (Lohmann

et al., 1999) and HCV cell culture systems (Lindenbach et al., 2005; Wakita et al., 2005; Zhong et al., 2005). The HCV-JFH1 strain, which is a genotype 2a clone derived from a Japanese fulminant hepatitis patient that can replicate efficiently in Huh7 cells (Kato et al., 2003; Kato et al., 2001), has contributed to the establishment of the HCV cell culture system. Furthermore, the Huh7-derived cell lines, Huh-7.5 cells, Huh-7.5.1, and Lunet cells allow production of higher viral titers and have a higher permissiveness for HCV (Koutsoudakis et al., 2007; Lindenbach et al., 2005; Zhong et al., 2005). The HCV-JFH1 cell culture system now allows us to study the complete HCV life cycle: virus–cell entry, translation, protein processing, RNA replication, virion assembly, and virus release.

HCV belongs to the family *Flaviviridae*. One of the characteristics of the *Flaviviridae* is that they cause cytopathic effects (CPE). The viruses have positive strand RNA genomes of ~10 kilobases that encode a polyprotein of ~3000 amino acids.

Abbreviations: HCV, hepatitis C virus; IFN, interferon; CPE, cytopathic effect; ER, endoplasmic reticulum; UPR, unfolded protein response; PFU, plaque-forming unit; FFU, focus-forming unit; RdRp, RNA-dependent RNA polymerase.

* Corresponding author. Department of Gastroenterology and Hepatology, Tokyo Medical and Dental University, 1-5-45 Yushima, Bunkyo-ku, Tokyo 113-8519, Japan. Fax: +81 3 5803 0268.

E-mail address: nsakamoto.gast@tmd.ac.jp (N. Sakamoto).

¹ Y.S. and N.S. contributed equally to this work.

The protein is post-translationally processed by cellular and viral proteases into at least 10 mature proteins. The viral nonstructural proteins accumulate in the ER and direct genomic replication and viral protein synthesis (Bartenschlager and Lohmann, 2000; Jordan et al., 2002; Mottola et al., 2002). It has been reported that Japanese encephalitis virus (JEV), bovine viral diarrhea virus (BVDV), and dengue viruses (DEN) cause apoptotic cell death (Despres et al., 1996; He, 2006; Jordan et al., 2002; Su et al., 2002). In addition, certain amino acid substitutions in the viral structural or nonstructural proteins affect the replication and cytopathogenicity of these viruses substantially (Blight et al., 2000; Maekawa et al., 2004; Mendez et al., 1998). It has been recently reported that HCV-JFH1-transfected Huh-7.5.1 cells died when all of the cells were infected and intracellular HCV-RNA reached maximum levels (Zhong et al., 2006). These findings suggest HCV-induced cytopathogenicity. However, the mechanisms have not been well documented.

In the present study, we investigated the cellular effects of HCV infection and replication using the HCV-JFH1 cell culture system. Here, we report that HCV-JFH1-transfected and infected cells show substantial CPE that are characterized by massive apoptotic cell death with the expression of several ER stress-induced proteins. Taking advantage of the CPE, we developed a plaque assay for HCV in cell culture and isolated subclones of HCV that showed enhanced replication and cytopathogenicity. We have demonstrated that these viral characters were determined by mutations at certain positions in the structural and nonstructural regions of the HCV genome, especially the NS5B region.

Results

Production of infectious HCV-JFH1 by JFH1-RNA transfected cells

After transfection of HCV-JFH1 RNA into Huh-7.5.1 cells, intracellular HCV RNA and HCV antigen were continuously detectable in the cell culture (Fig. 1A). Furthermore, the culture supernatant from the transfected cells was positive for core protein, which reached maximum levels at 14 days post-transfection and was continuously detectable during the cell culture (Fig. 1A, black bar). The culture supernatant was readily infectable to naive Huh-7.5.1 cells (data not shown). Immunofluorescence assay showed that 48% of the JFH1-RNA-transfected cells and 42% of the virus-infected cells were positive for HCV core protein. These results demonstrate that the transcript of HCV-JFH1 clone replicates efficiently and produces infectious virus particles in cells, as reported previously (Wakita et al., 2005; Zhong et al., 2005).

Hepatitis C virus infection induced cytopathic effects in vitro

By the seventh day post-transfection, the production of virus decreased concomitant with massive cell death and then cell growth gradually recovered. At 14–16 days post-transfection, the levels of HCV-RNA and core antigen reached maximum (Fig. 1). In the JFH1 mutants JFH1/GND and JFH1/ Δ E1-E2-RNA-transfected Huh-7.5.1 cells, the viral replication and host cell death were not observed. The massive cell death after HCV-

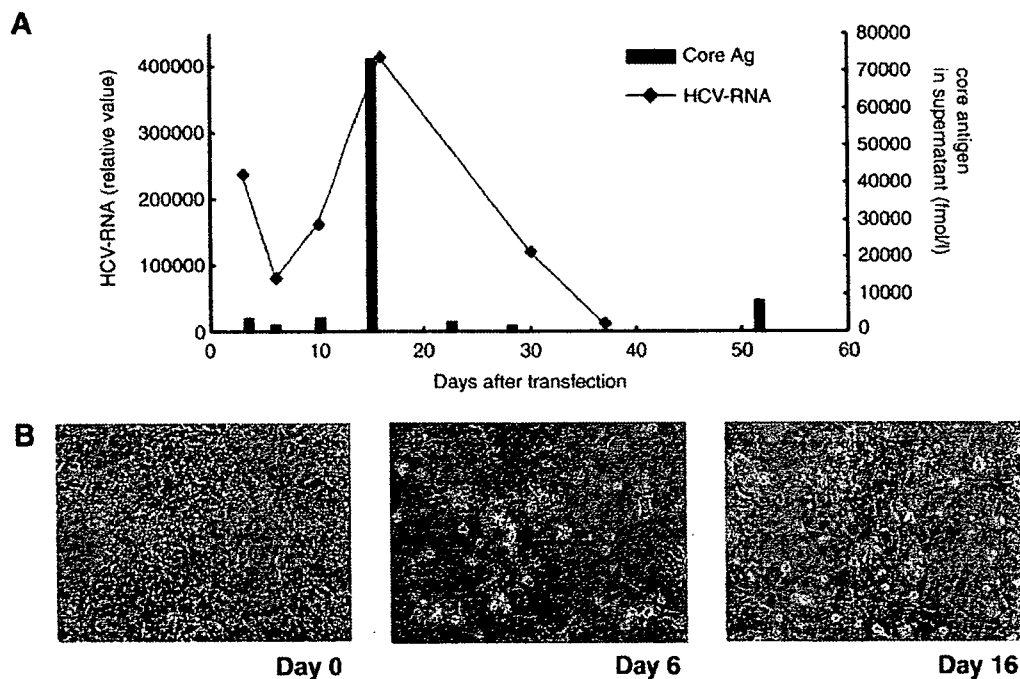


Fig. 1. Replication of HCV-JFH1 RNA in JFH1-transfected and infected Huh-7.5.1 cells. (A) Levels of HCV-RNA in JFH1 RNA-transfected cells. After transfection of the *in vitro* transcribed JFH1-RNA into Huh-7.5.1 cells, total cellular RNA was isolated on indicated days and quantified by real-time RT-PCR. Furthermore, the culture supernatant of JFH1-RNA transfected Huh-7.5.1 cells was collected on the days indicated and the levels of core antigen in the culture supernatant were measured (black bar). (B) HCV-JFH1-transfected Huh-7.5.1 cells (the left panel, day 0; the middle panel, day 6; the right panel, day 16).